



Aerospace Combustion

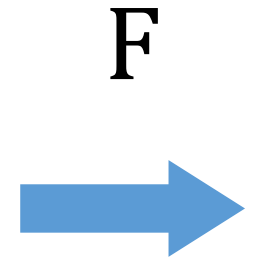
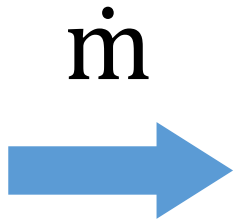
Lecture 14:

Combustion Chamber Design



Introduction

c_{eff} → Effective exhaust velocity

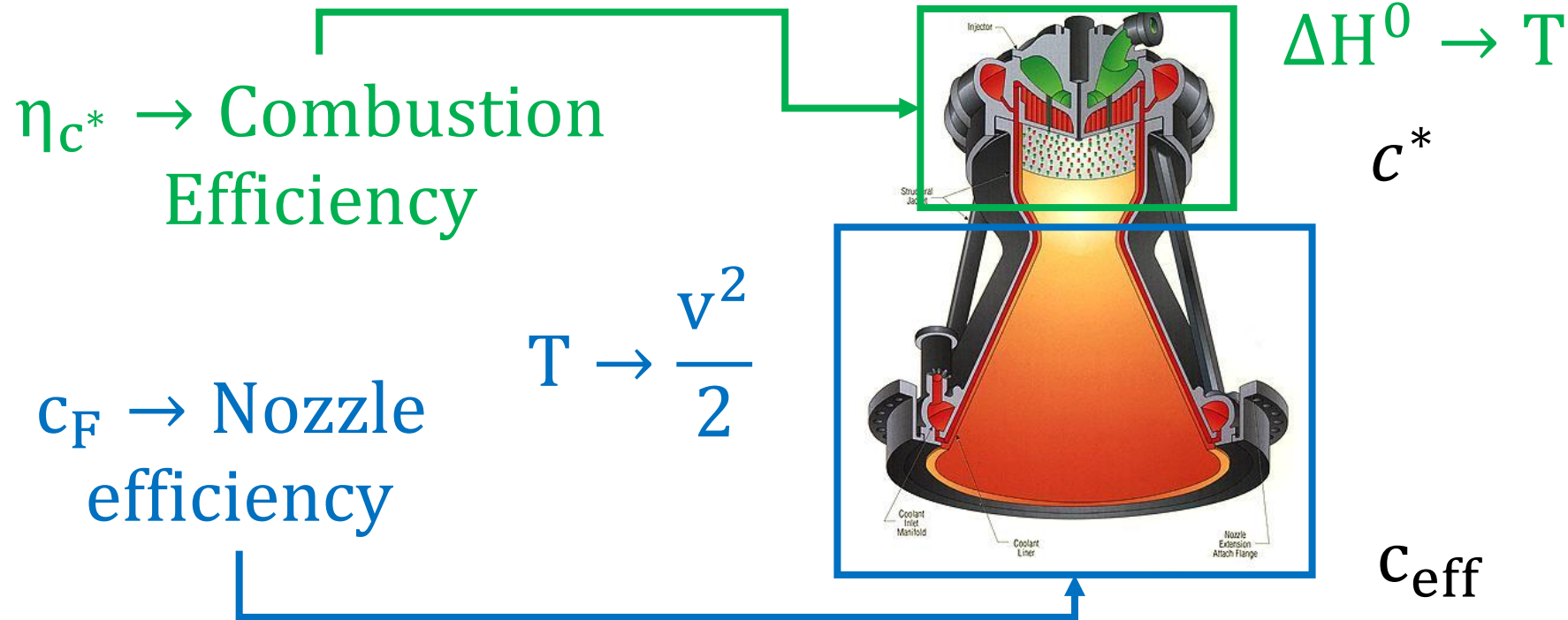


$$c_{\text{eff}} = \frac{F}{\dot{m}}$$

Raptor engine fire test, Credit: 

How well we convert kg/s to Newtons

$$C_{eff} = c_F \underbrace{\eta_c^* c_{id}^*}_{c^*}$$



Combustion Chamber Requirements

Complete the following processes to reach desired **effective exhaust velocity**:

- Atomization and Vaporization
- Mixing
- Combustion

Performance

- **Minimal dry weight**

Cost

- Minimize the economical cost

Structural:

- Endure a given number of thermal cycles

Expendable (5 cycles)

Moderate reusable (30 cycle)

Highly reusable (>100 cycles)

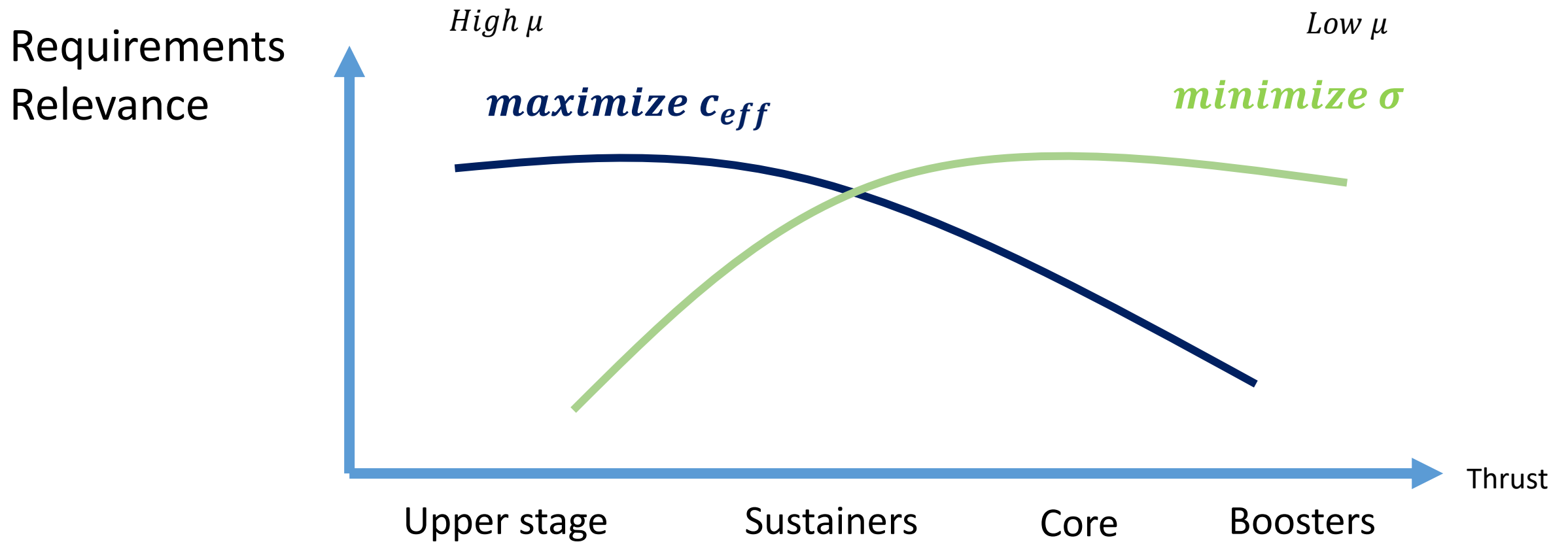
$$\Delta v = c_{eff} \log \left(\frac{1}{\mu + \sigma} \right)$$

$$\sigma = \frac{\textit{structural mass}}{\textit{total mass}} \in [0.1 - 0.2]$$

$$\mu = \frac{\textit{payload mass}}{\textit{total mass}} \in [0.005 - 0.05]$$

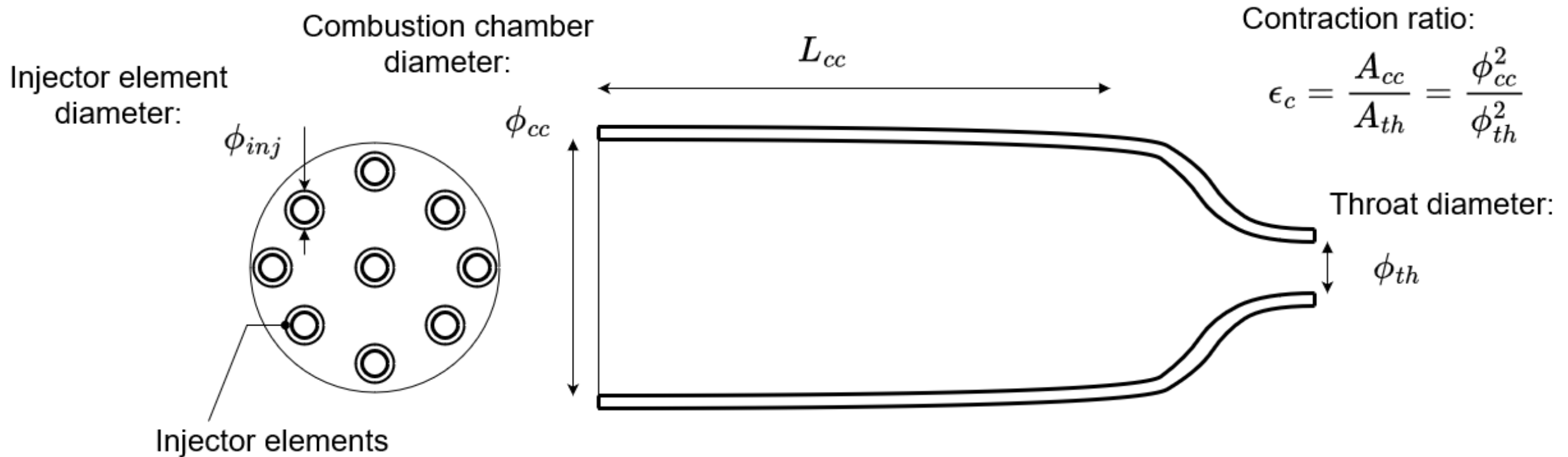
Requirements

Depending on the application, the relevance of the requirements varies



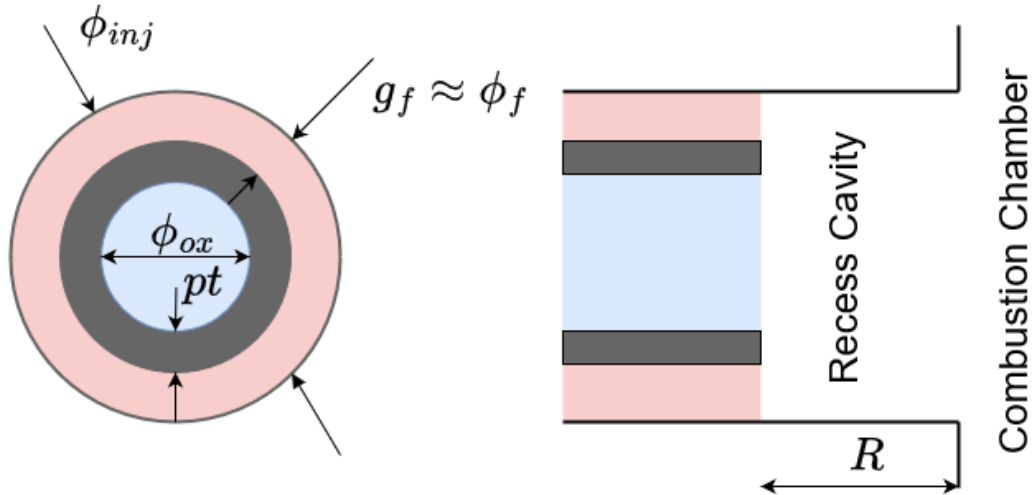
Combustion chamber geometry (I)

Tubular combustion chamber:



Combustion chamber geometry (II)

Coaxial injector



Injection posttip:

pt

Fuel gap:

g_f

Oxidizer diameter:

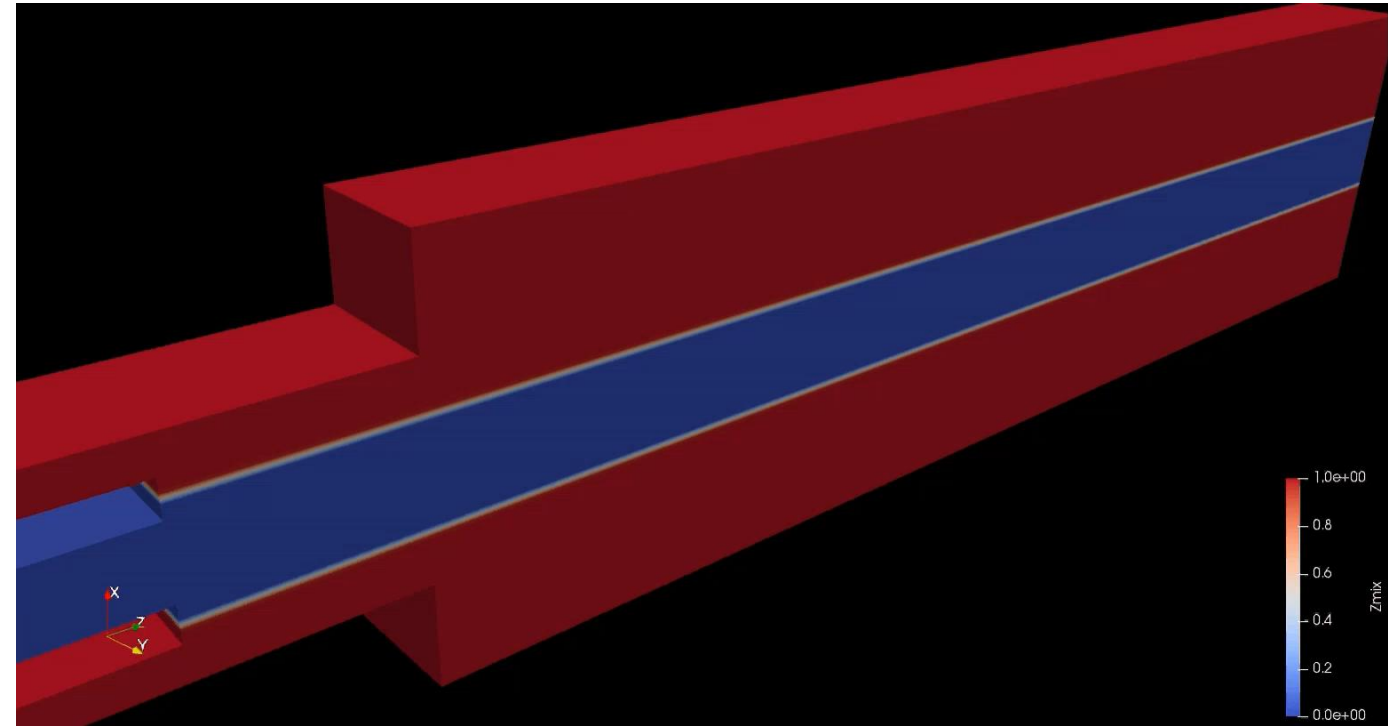
ϕ_{ox}

Injector diameter:

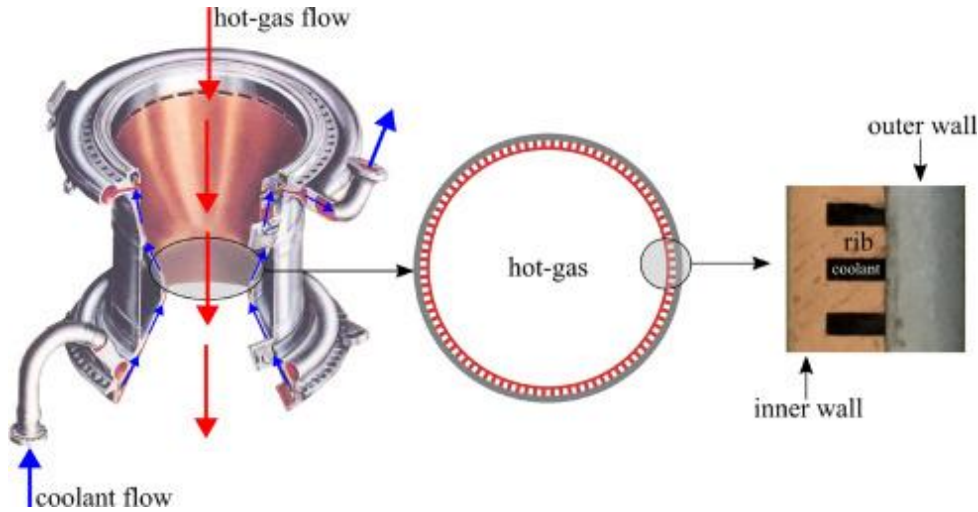
ϕ_{inj}

Recess length:

R



Combustion chamber geometry (III)



Pizzarelli et al. 2023

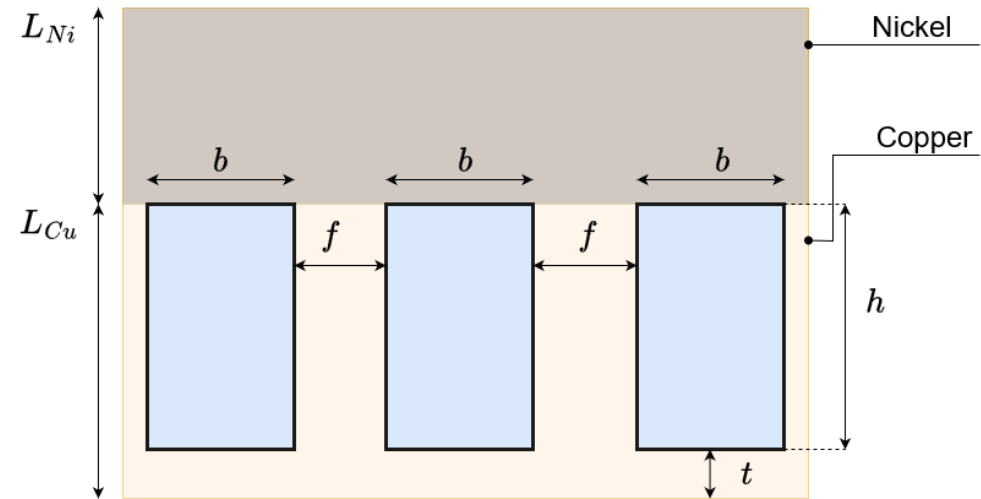
Hydraulic diameter of a rectangular duct:

$$\phi_H = 4 \frac{\text{Area}}{\text{Perimeter}} = \frac{bh}{2(b+h)}$$

$$L_{Cu} + L_{Ni} \ll \phi_{CC}, \rightarrow$$

Geometry can be approximated neglecting arcs:

Cooling fins/ribs:
 f
 Cooling channel
 width:
 b
 Cooling channel
 height:
 h



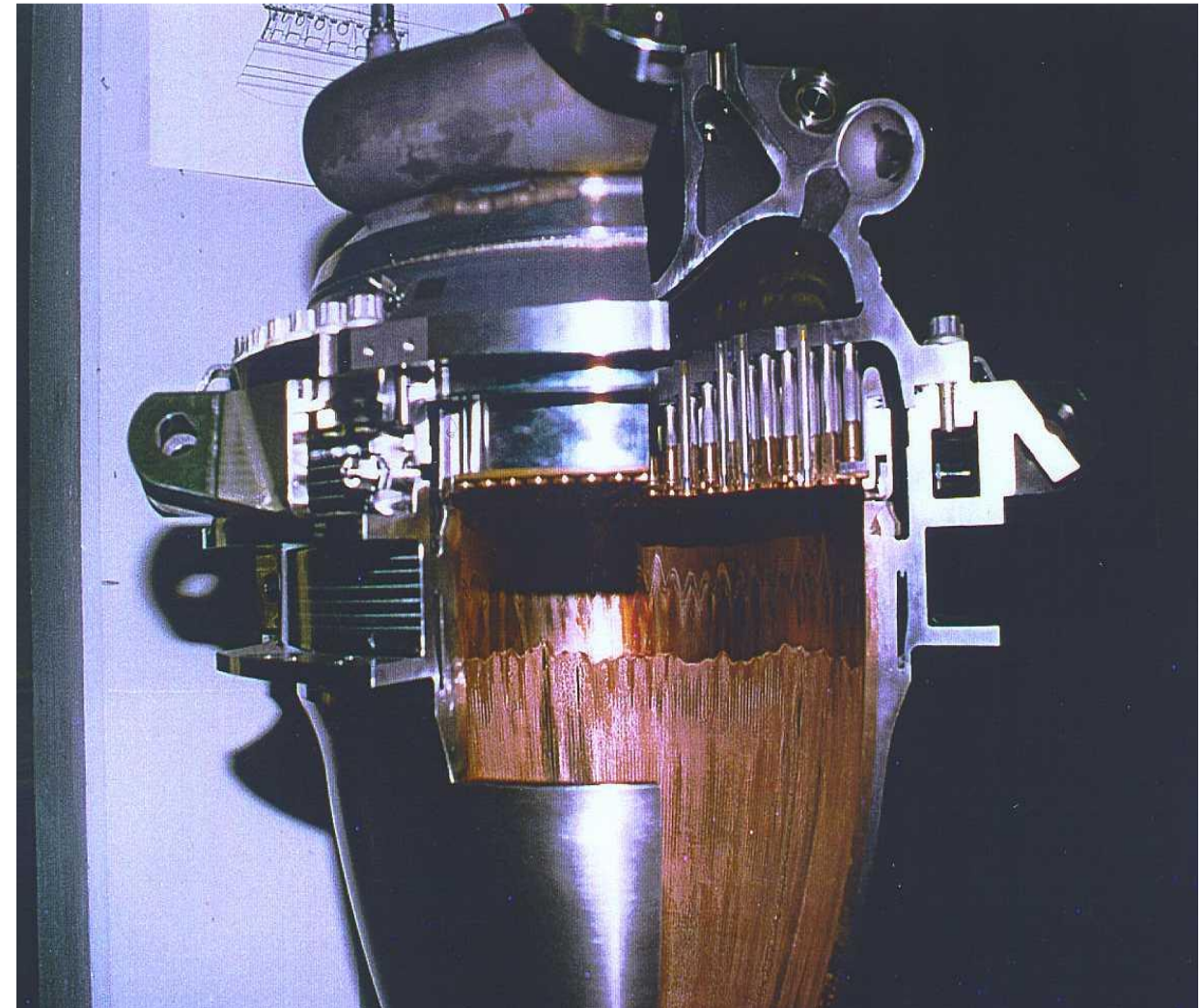
$$m_{CC} \approx L_{CC} \left(\rho_{Cu} \left((h+t) \phi_{CC} \pi \left(1 - \frac{bh}{L_{Cu}(b+f)} \right) \right) + \rho_{Ni} (L_{Ni} \phi_{CC} \pi) \right)$$



Injection

Injector System Requirements

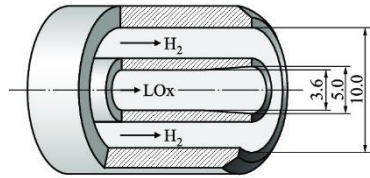
- Acoustic decoupling of propellant supply and distribution domes and combustion chamber
- Homogeneous distribution of propellant mass flow rates
- Optimum atomization, distribution and mixing of propellants
- Minimum interaction with combustion chamber wall
- Avoidance/Damping of combustion instabilities
- Mechanical integrity to transient pressure loads
- Thermal integrity towards heat loads



Vulcain 1 combustion chamber: Courtesy: ASTRIUM EADS Ottobrunn

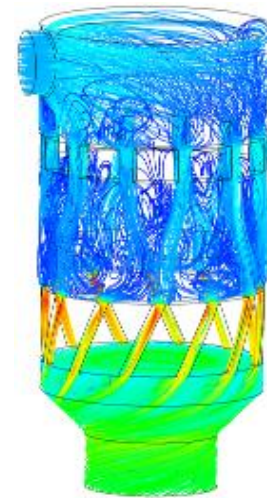
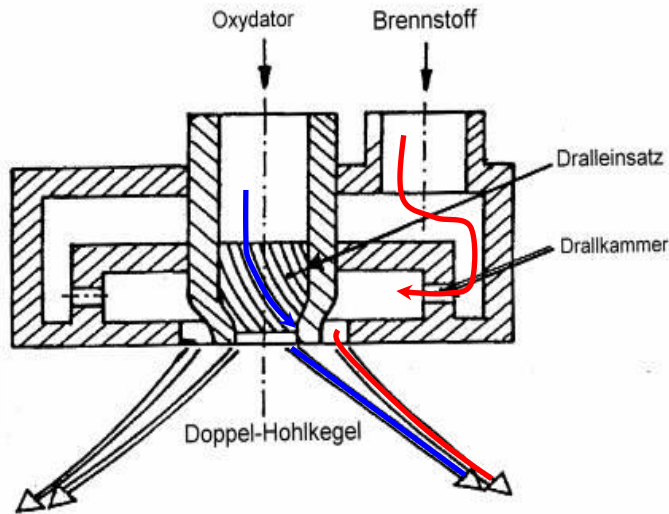
Injector Typologies

- Coaxial Injection

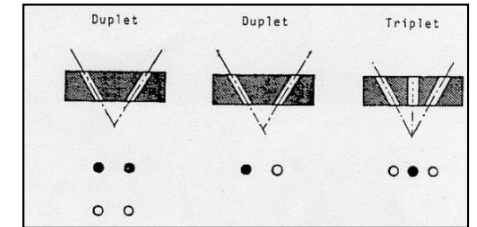


Pohl et al. 2013

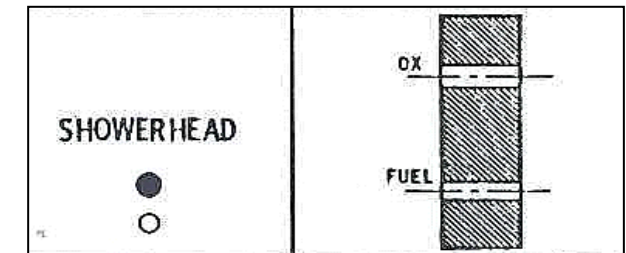
- Swirl Injection



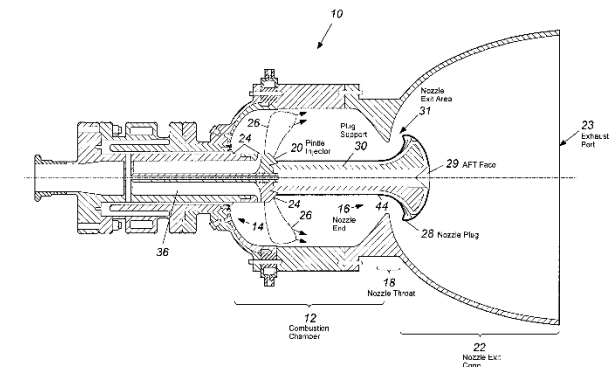
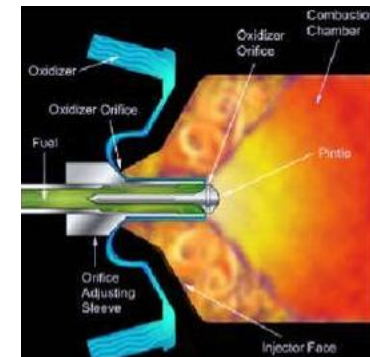
- Impinging Injection



- Showerhead Injection

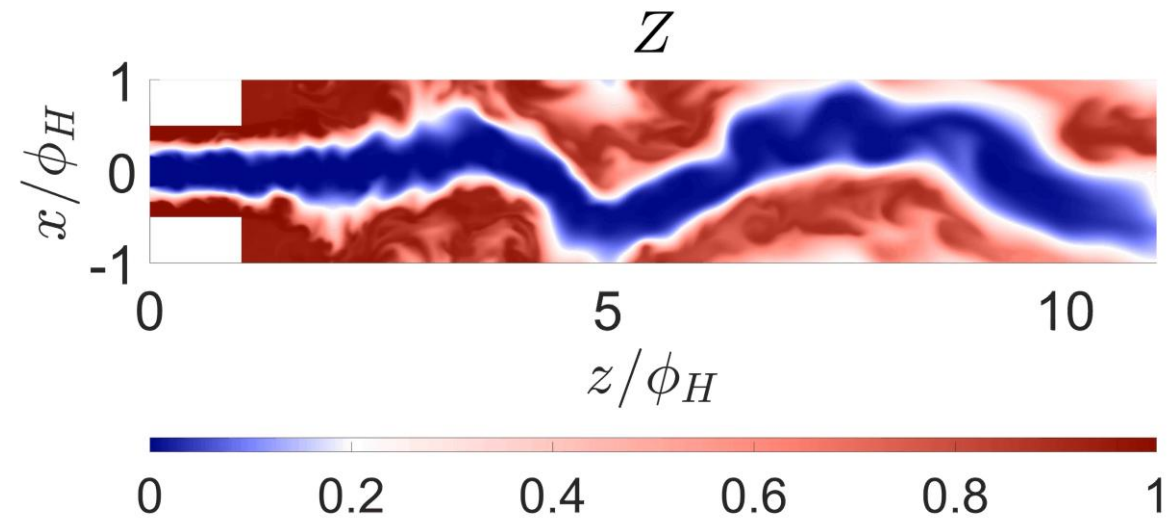
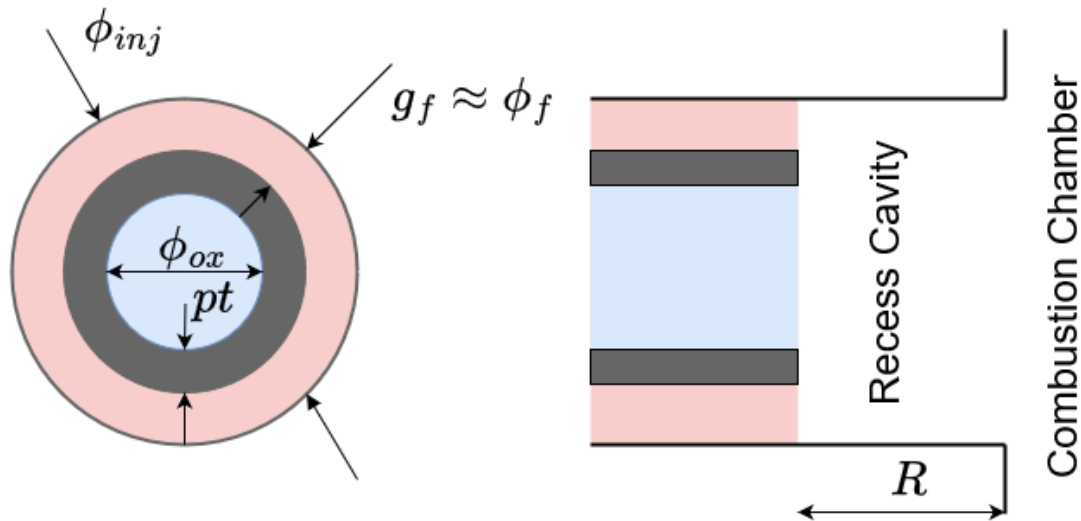


- Pintle



Coaxial Injection

- Mixing due to turbulence created by aerodynamic destabilization at the shear layer
- Highly applicable to cryogenic propellants; today's standard for LOX/LH2
- **In combination with swirl and impinging principle** well applicable for storable propellants (MMH/N2O4)
- Good scalability
- Excellent combustion efficiency



Coaxial Injection

- Velocity ratio VR

VR > 10 or VR < 0.1 are desired to increase velocity shear and promote turbulent mixing

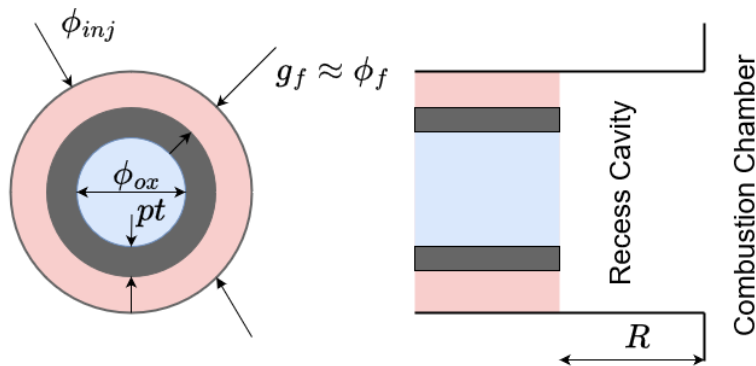
For very high VR (VR > 100 or VR < 0.01), combustion may become unstable and flame anchoring fragile.

- O/F

In many cases is constant for all elements, but sometimes it may be adapted to have smaller O/F near the wall and reduce oxidation risk.

- R

Injection recess increases combustion efficiency and stability. Almost every modern coaxial injector has a recess length in the order $R/\phi_{inj} \in [0.5, 2]$.



$$VR = \frac{v_{ox}}{v_f}$$

$$J = \frac{\rho_{ox} v_{ox}^2}{\rho_f v_f^2} = \frac{\rho_{ox}}{\rho_f} VR^2$$

$$\frac{O}{F} = VR \cdot \rho_R \cdot A_R$$

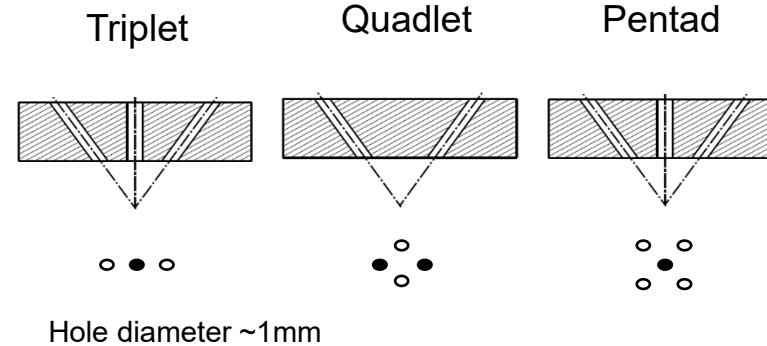
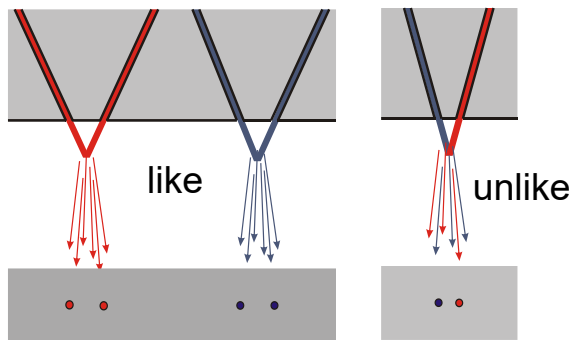
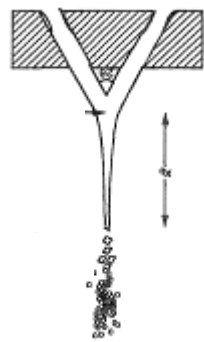
Swirl Injection

- Injector geometry induces rotational motion of propellant.
- Good atomization and mixing results in high efficiencies at small mass flow rates (single element thruster)
- Recirculation increases flame stability.
- Generation of stable coolant film.
- Strong coupling between efficiency and wall heat loads.
- In Russia applied to multi-element systems. Almost all LOX/kerosene engines apply this injection concept
- Sensitive to fabrication tolerances, manufacturing precision and pollution.

Impinging Injection

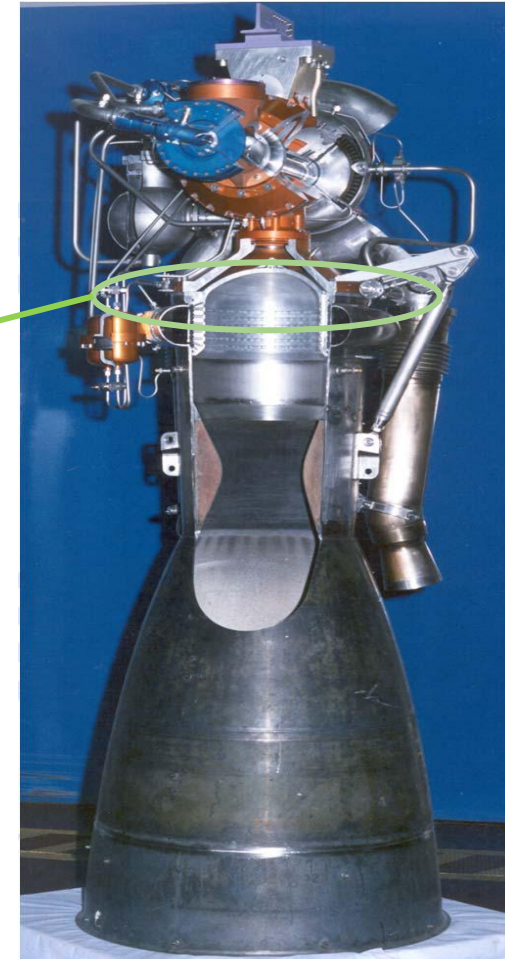
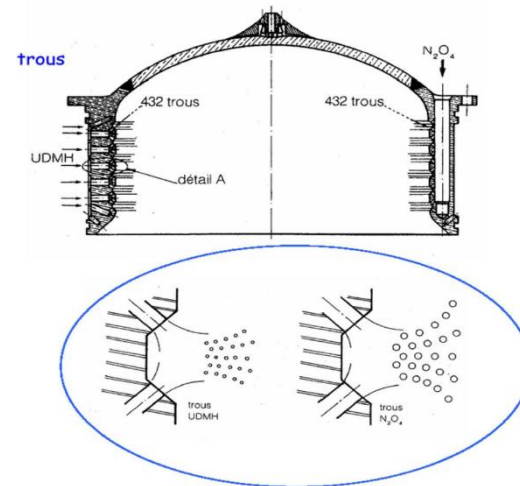
- Highly applicable to poorly vaporizing propellants (e.g. MMH/N₂O₄. in USA used for LOX/RP1)
- High combustion efficiency
- Sensitive to fabrication tolerances and tendency combustion instabilities
- Preferably used for liquid/liquid

many variants possible



Impinging Injection: Use Case, Viking

- Injection along side walls, film cooled wall and throat
- Similarities with German A4 and early Russian engines
- Strong sensitivity to develop combustion instabilities
- After a failure flight (Ariane 1, flight 23) propellant was slightly modified and manufacturing tolerances increases to reduce instabilities.



Showerhead Injection

- Axial propellant injection with no aerodynamic assisted atomization (jet turbulence and natural instability); propellant mixture quality defined by geometry
- Low heat load of injector front plate and combustion chamber wall
- Poor propellant mixing and combustion efficiency
- High performance requires either small holes or large contraction ratios (lengths)
- Performance nearly constant for large operational range (throttling)
- Simple design but difficult to manufacture (if $d < 1$ mm)

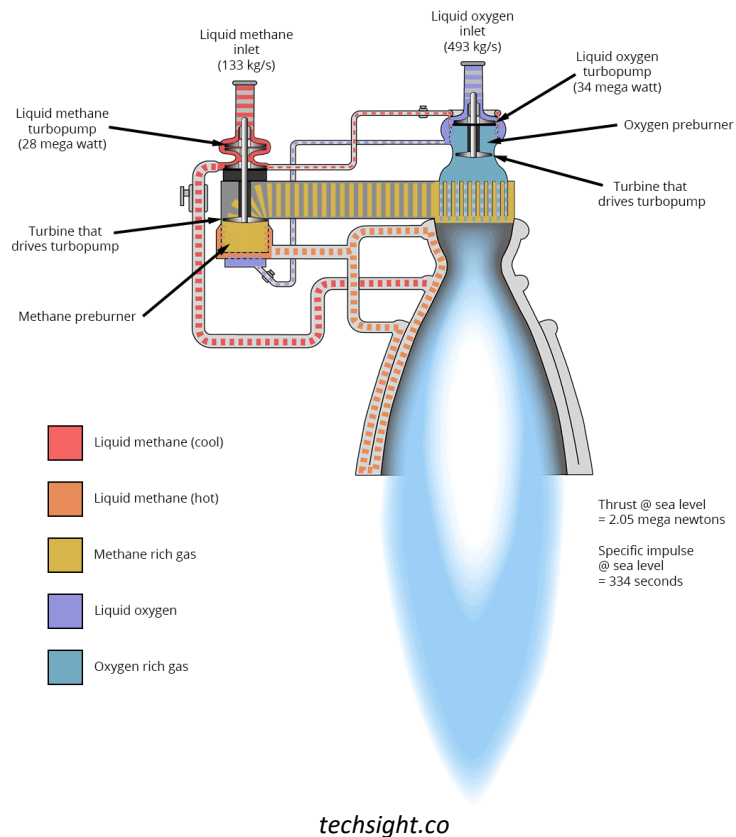




Heat Loads and Cyclic Fatigue

Cooling

Regenerative cooling of raptor



- In rocket engines, typical equilibrium temperatures of the combustion products are in the order of 3000-3500, well above the melting point of typical alloys.
- A cooling mechanism is needed to obtain wall temperatures that ensure structural integrity for the planned number of cycles.
- Regenerative cooling is a common solution used in engines with $p > 20$ bar. The fuel is used as coolant before burning it in the combustion chamber.
- For $p > 120$ film cooling is often used together with regenerative cooling, especially in kerosene engines.

Convective heat transfer

- In a flow with different temperature between the walls and the fluid, a heat flux is formed. This heat flux can be defined using the heat transfer coefficient α [W/m^2K]:

$$\dot{q} = \alpha \Delta T \rightarrow \begin{cases} \text{Cooling: } \Delta T = T_{wall} - T_{fluid} \\ \text{Heating: } \Delta T = T_{fluid} - T_{wall} \end{cases}$$

- If the flow is laminar, the film coefficient is roughly:

$$\alpha \sim \lambda / \phi$$

- In a turbulent flow, the presence of vortices enhances the heat transfer coefficient. The Nusselt number measures how large is the heat transfer coefficient compared to the laminar case:

$$Nu = \frac{\alpha}{\alpha_L} = \frac{\alpha}{\lambda} \phi$$

The Nusselt number is modelled with semi-empirical formulas. Most formulas contain a quasi-linear dependency on the Reynolds number:

$$Nu \sim Re^n, n \in [0.7 \ 1]$$

Convective heat transfer: Nusselt number at the hot gas side

Empirical Relations
 of Bartz -type:

$$Nu = 0.062 Re^{0.8} Pr^{0.3} \quad \text{with} \quad \begin{aligned} Re &\approx 10^7 - 10^8, \\ Pr &\approx 0.5 \end{aligned}$$

Modified
 Bartz:

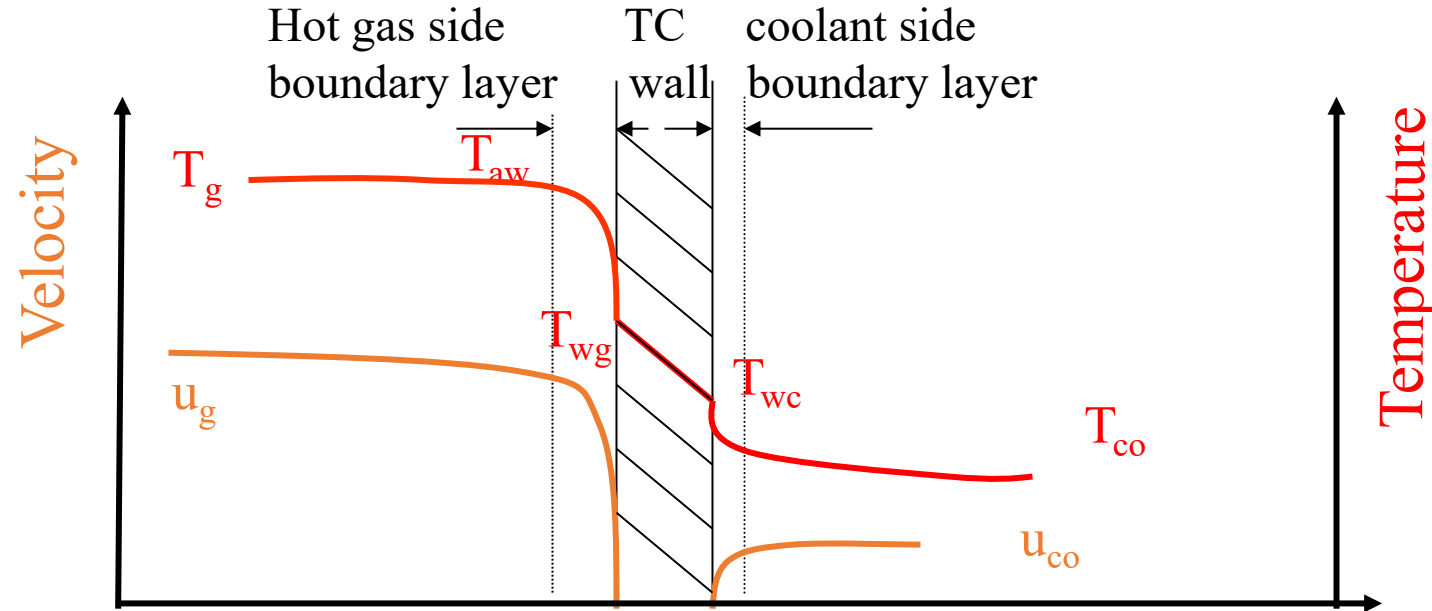
$$\alpha_g = \left[\frac{0.026 \left(\frac{\mu^{0.2} C_p}{Pr^{0.6}} \right)_{ns} \left(\frac{(p_c)_{ns} g}{c^*} \right)^{0.8} \left(\frac{D_t}{R} \right)^{0.1}}{D_t^{0.2}} \right] \left(\frac{A_t}{A} \right)^{0.9} \sigma$$

with

$$\sigma = \frac{1}{\left[\frac{1}{2} \frac{T_{WG}}{(T_c)_{ns}} \left(1 + \frac{k-1}{2} Ma^2 \right) + \frac{1}{2} \right]^{0.68} \left[1 + \frac{k-1}{2} Ma^2 \right]^{0.12}},$$

$$Pr = \frac{4k}{9k-5}, \quad \text{and} \quad \mu = \left(46.6 \cdot 10^{-10} \right) M^{0.5} T^{0.6}$$

Convective heat transfer: Nusselt number of the cooling channel



Bartz-type Equations: $Nu = K Re^a Pr^b$, $Re \approx 10^6 - 10^7$, $Pr \approx 1$

	K	a	b	
Methane:	0.0023	0.8	0.4	
Propane:	0.005	0.95	0.4	
Kerosene:	0.005	0.95	0.4	for $Re < 2 \cdot 10^4$
	0.023	0.8	0.4	for $Re > 2 \cdot 10^4$
LH2	0.062	0.8	0.3	

Convective heat transfer: Nusselt number of the cooling channel

- Improved Relations:

$$Nu = K Re^a Pr^b \left(\frac{T_w}{T_b} \right)^n \left(1 + \frac{2D}{L} \right)^m$$

$$Nu = K Re^a Pr^b \left(\frac{\rho}{\rho_w} \right)^c \left(\frac{\mu}{\mu_w} \right)^d \left(\frac{k}{k_w} \right)^e \left(\frac{\bar{c}_p}{c_p} \right)^f \left(\frac{p}{p_{cr}} \right)^g \left(1 + \frac{2D}{L} \right)^m$$

Fuel	P_c MPa	U_{ch} m/s	q MW/m ²	T_b K	T_w K	K	a	b	c	d	e	f	g	m	n
C ₂ H ₆	13.7	6-30		420-810		0.00538	0.80	0.4	-0.125	0.242	0.193	0.395	-0.024	1	0
	3-12.4	15-45	0.3-16.4	120-395		0.00545	0.90	0.4	-1.1	0.23	0.27	0.53	0	1	0
	7-13.8	30-60	3.1-18.2	230-300	230-810	0.0280	0.80	0.4	0	0	0	0	0	0	0
						0.00696	0.88	0.5	0	0	0	0	0	0	-1.0
CH ₄	27-34	55-238	2.6-139	146-275		0.0220	0.80	0.4	0	0	0	0	0	0	-0.45
	27-34	55-238	2.6-139	146-275		0.0230	0.80	0.4	0	0	0	0	0	0	-0.57
	7-13.8	30-60	3.1-18.2	230-300	230-810	0.0230	0.80	0.4	0	0	0	0	0	0	0
						0.0230	0.80	0.4	0	0	0	0	0	0	-0.80
RP-1	7-13.8	30-60	3.1-18.2	230-300	230-810	0.0440	0.76	0.4	0	0	0	0	0	1	0
	7-13.8	30-60	3.1-18.2	230-300	230-810	0.0068	0.94	0.4	0	0	0	0	0	0	0
						0.0056	0.90	0.4	0	0	0	0	0	0	0

Heat transfer predictions

The model modifications account for

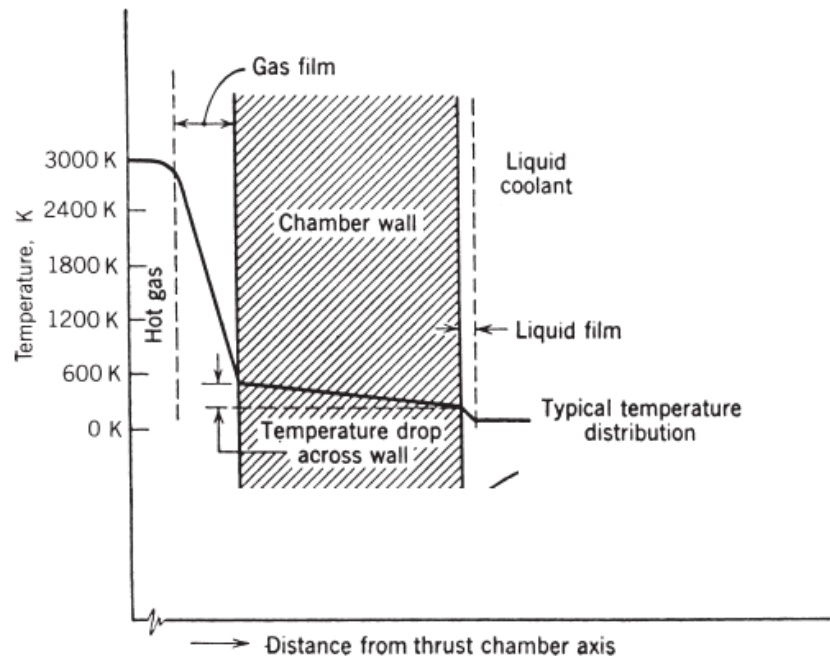
- Chamber geometry (injector wall distance, contraction ratio, curvatures)
- Cooling channel entrance, exit and geometry (aspect ratio) effects
- Chamber material properties (catalytic effects, variable heat conduction, ...)
- Fluid properties (near-critical effects, pyrolysis, ..)
- Others (measuring techniques, facilities,)

They all have to be adjusted by experimental data since deviations are typically of the order

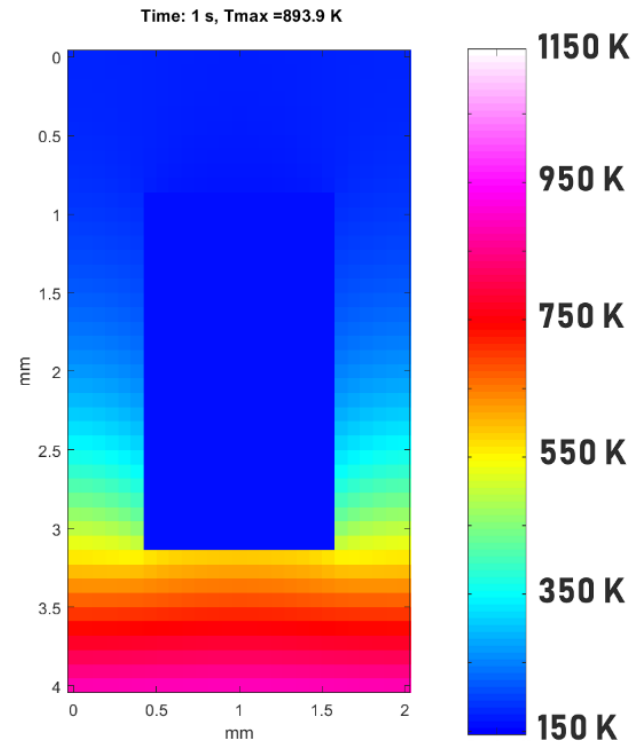
$$\frac{Nu_{exp.}}{Nu_{cal}} = 1 \pm 0.2$$

Regenerative cooling

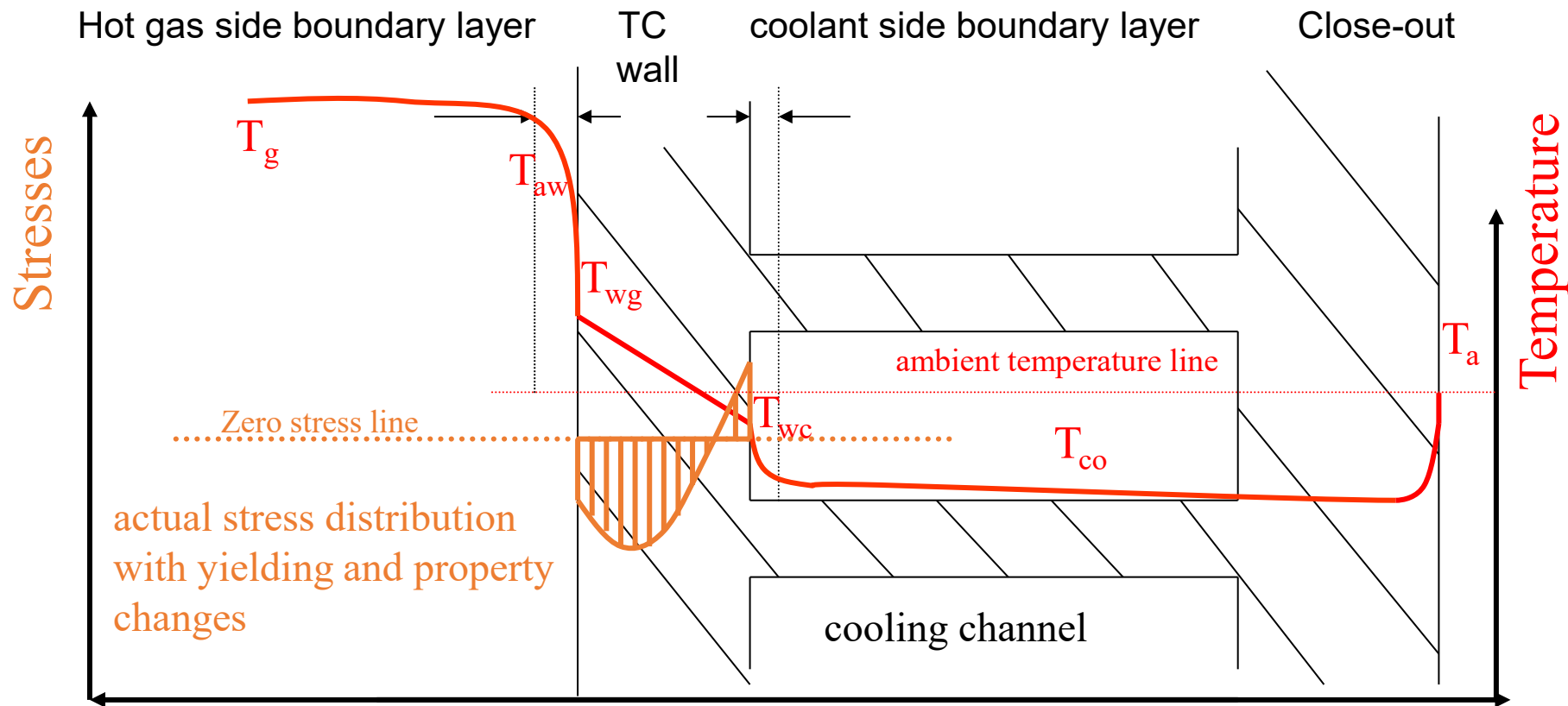
Typical 1D temperature profile



Typical 2D temperature profile



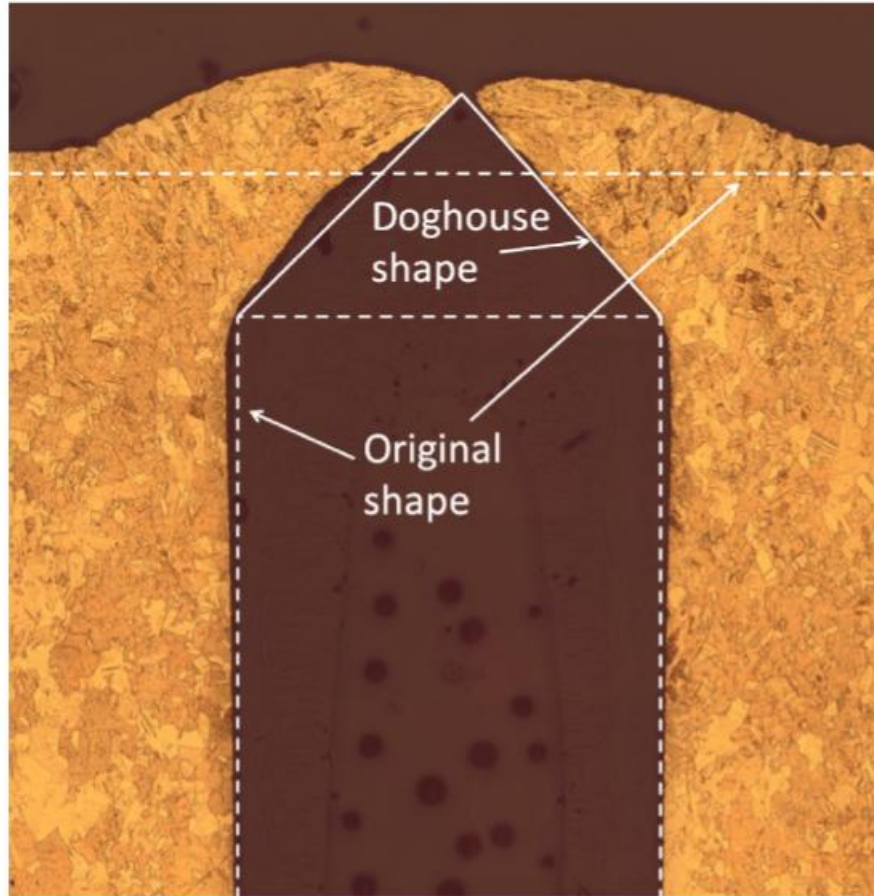
Convective heat transfer



- Due to thermal dilatations, temperature gradients produce deformations and stresses.
- When the engine is cooled down, the plastic component of the deformation remains.
- Over multiple cycles, these plastic deformations accumulate, leading to an eventual structural failure.

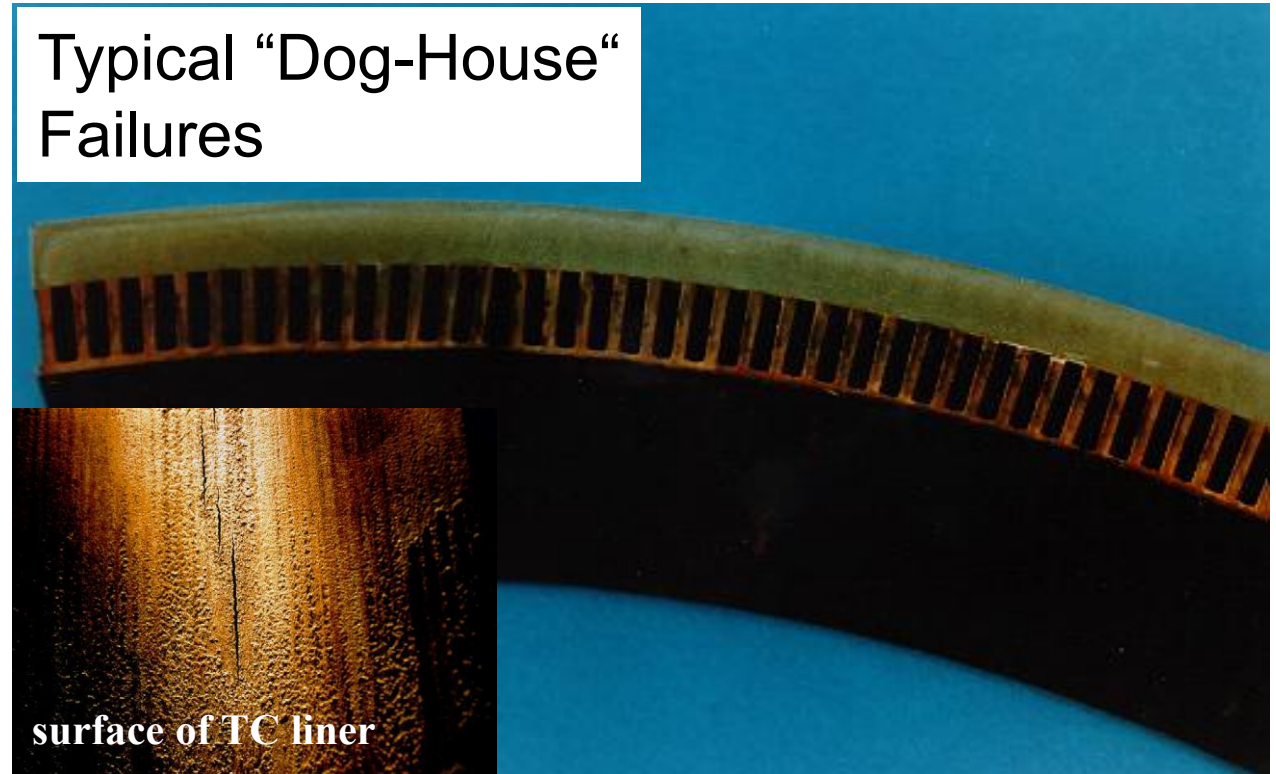
- Start-up and shut-down transients are most severe
- Thermal induced plastic deformations in RP-1/ LOX or storable engines are typically lower due to reduced temperature differences

Convective heat transfer



- The cumulative effect of thermal strain produces the so-called doghouse effect, which eventually leads to structural failure.

Typical “Dog-House” Failures



Cyclic fatigue: Simplified approach

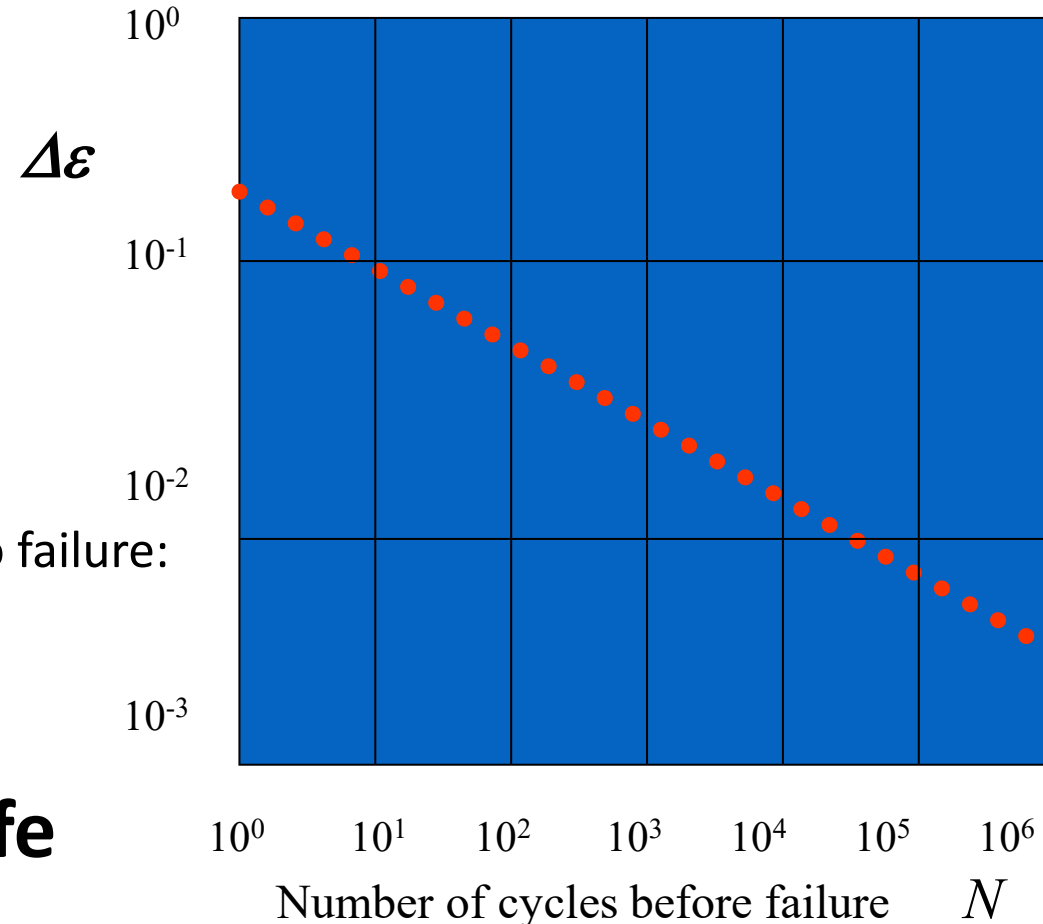
Additional plastic deformation per cycle $\Delta\varepsilon$:

$$\Delta\varepsilon \sim \dot{q} \sim T_{wall}^n$$

$$n \in [0.6, 1]$$

Simple empirical modelling of number of cycles to failure:

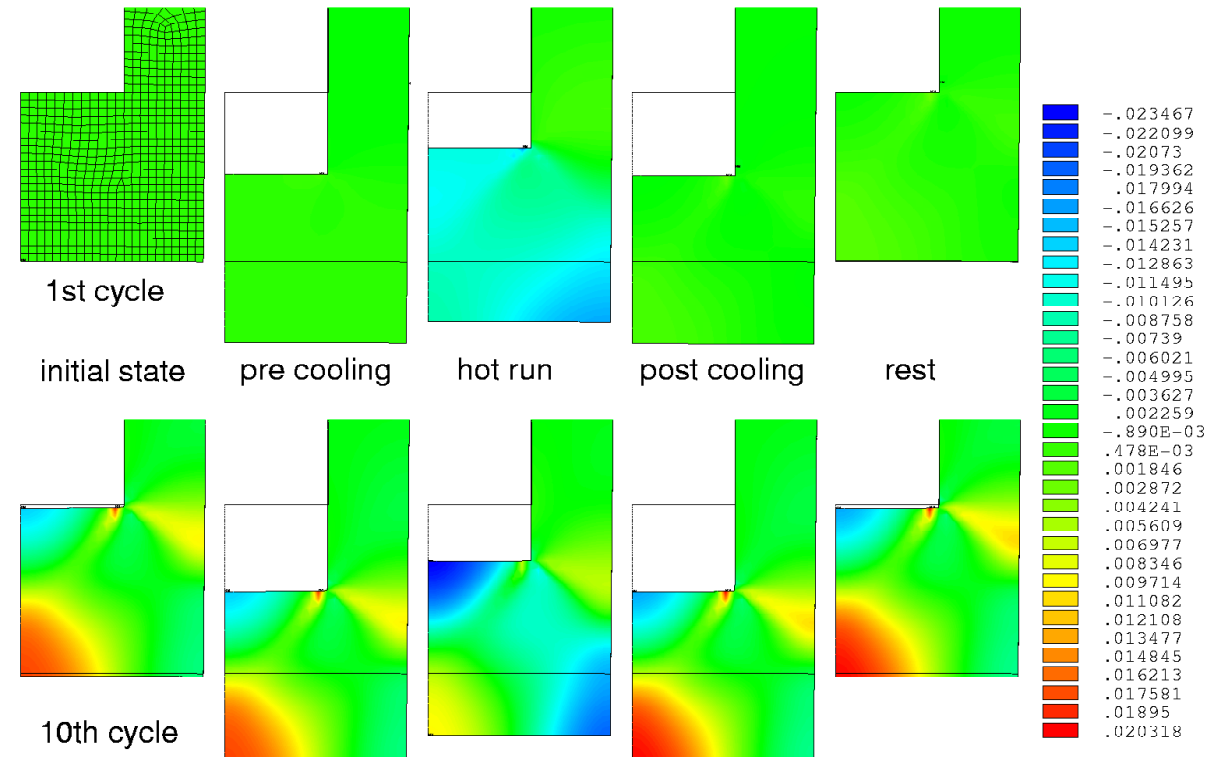
$$N = A + B \log(\Delta\varepsilon)$$



Low wall temperature \leftrightarrow Long life

Cyclic fatigue: Modern approach

- The problem is solved with Finite Elements in 2 or 3D to obtain the field of deformations.
- For 3D conjugate FEM – CFD
- A damage value is obtained depending on the accumulated strain. Failure occurs when the point with largest damage surpasses the critical value.



Thermal cycles and flights

Expendable use (1 Flight)

- Test after manufacturing
- Test after launcher integration
- Actual flight

Each of these activities requires two thermal cycles, 1 for the real firing and other for the case of abort.

Total: 6 thermal cycles

Moderate reusability (5-10 Flights)

- Test after manufacturing
- Test after launcher integrations
- Actual flights

The manufacturing test only happens once, and it is statistically unlikely that aborts are required frequently. The probability of abort has to be determined with appropriate safety margins. The relationship between thermal cycles and flights can be estimated as:

$$N_{thermal} = 6 + \left(\frac{1}{1 - P(Launch\ test\ abort)} + \frac{1}{1 - P(Launch\ abort)} \right) (N_{flights} - 1) \geq 6 + 2(N_{flights} - 1)$$

Thermal cycles and flights

Reusability (>100 Flights)

- Test after manufacturing become negligible
- Test after launcher integration
- Actual flight

The number of activities is large enough to apply continuous statistical theory. A detailed stochastic analysis is required to obtain an accurate estimation of the relationship between thermal cycles and flights:

$$N_{thermal} = \left(\frac{1}{1 - P(Launch\ test\ abort)} + \frac{1}{1 - P(Launch\ abort)} \right) N_{flights} \geq 2N_{flights}$$

Critical point

- The heat loads scale with:

$$\dot{q} \sim Re^{0.8}$$

Maximal heat loads \leftrightarrow Maximal Reynolds number

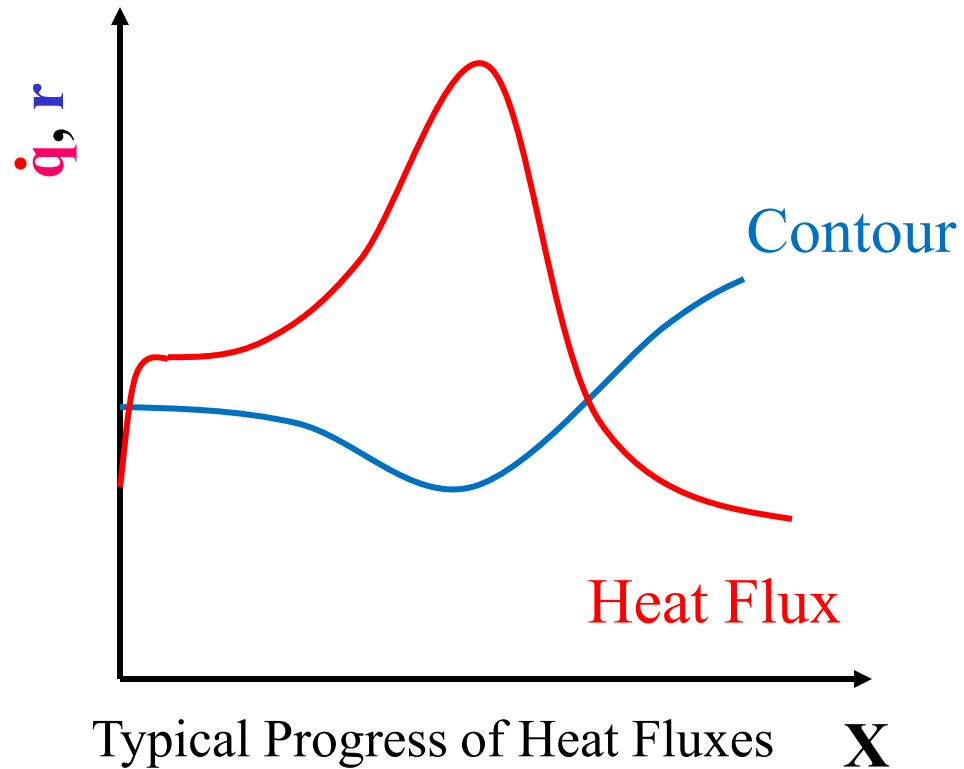
- For continuity we know:

$$\dot{m} = u\rho A = u\rho \frac{\pi}{4} \phi^2 = \text{constant}$$

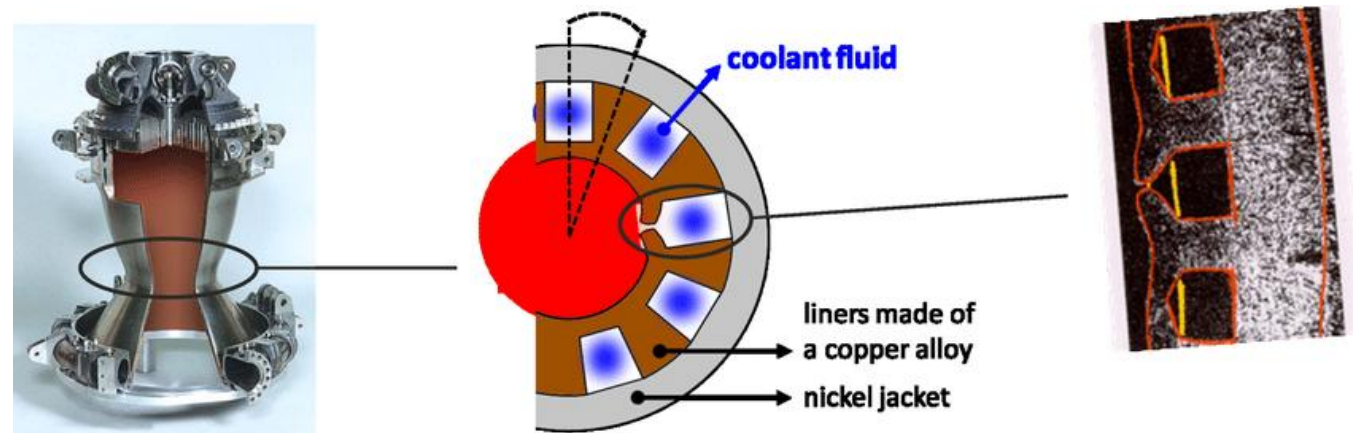
$$Re = \frac{u\rho\phi}{\mu} = \frac{4\dot{m}}{\pi\mu\phi} \rightarrow \text{Maximum Reynolds number at the throat!}$$

Engines always break at the throat, where the heat loads are maximal.

Critical point

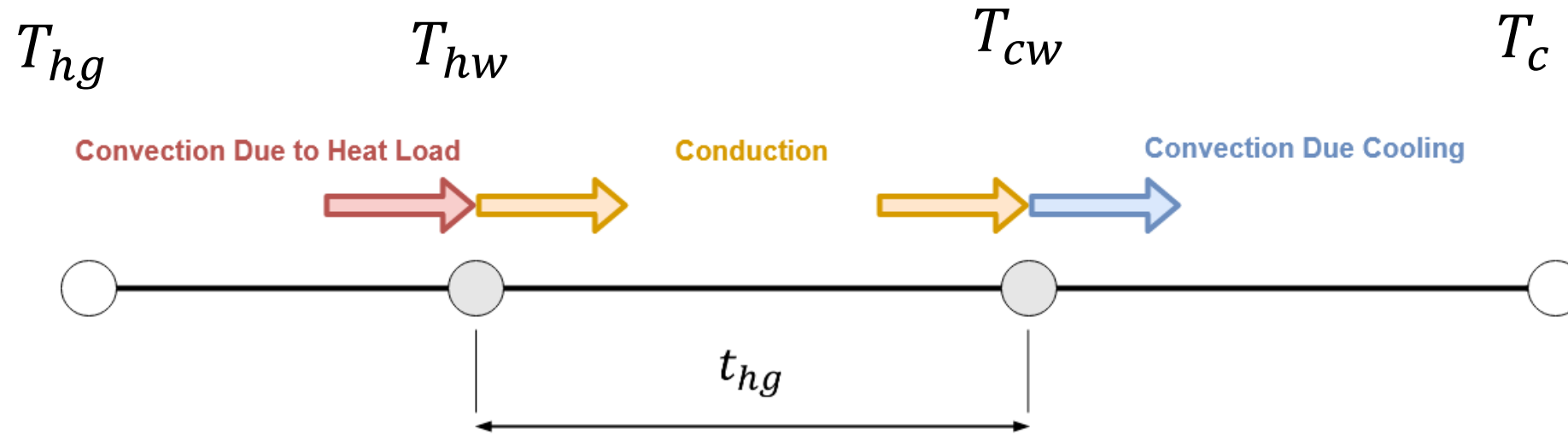


Thermo mechanical failure occurs almost always at the throat.



Fassin et al. 2016

1D Simplification



$$\dot{q} = \dot{q}_{conv,gas-hot\ wall} = \dot{q}_{cond} = \dot{q}_{conv,cool\ wall-cooling\ chanel}$$

Neglecting radiative heat transfer, cooling fins, and assuming constant thermal conductivity λ :

$$\begin{aligned} \dot{q} &= \alpha_{hg}(T_{hg} - T_{hw}) \\ \dot{q} &= \lambda \frac{T_{hw} - T_{cw}}{t} \\ \dot{q} &= \alpha_c(T_{cw} - T_c) \end{aligned}$$

1D Simplification

Unknowns (Outputs)

$$\dot{q} = \alpha_{hg}(T_{hg} - T_{hw})$$

$$\dot{q} = \lambda \frac{T_{hw} - T_{cw}}{t}$$

$$\dot{q} = \alpha_c(T_{cw} - T_c)$$

Known (Inputs)

$\alpha_c \rightarrow$ Given by turbulent flow at the cooling channel

$\alpha_{hg} \rightarrow$ Given by turbulent flow at the combustion chamber

$T_c \rightarrow$ Controllable property

$T_{hg} \rightarrow$ Given by the equilibrium temperature of the combustion products

$\lambda \rightarrow$ Material property

$t \rightarrow$ Manufacturing and design

$$T_{hw} = \frac{(\alpha_{hg} + \frac{t}{\lambda} \alpha_{hg} \alpha_c) T_{hg} + \alpha_c T_c}{\alpha_c + \frac{t}{\lambda} \alpha_{hg} \alpha_c} = \frac{(1 + \frac{t}{\lambda} \alpha_c) T_{hg} + \frac{\alpha_c}{\alpha_{hg}} T_c}{\frac{\alpha_c}{\alpha_{hg}} + \frac{t}{\lambda} \alpha_c}$$

$$T_{cw} = \frac{t}{\lambda} \alpha_{hg} T_{hg} + \frac{(1 + \frac{t}{\lambda} \alpha_c) T_{hg} + \frac{\alpha_c}{\alpha_{hg}} T_c}{\frac{\alpha_c}{\alpha_{hg}} + \frac{t}{\lambda} \alpha_c} \left(1 - \frac{t}{\lambda} \alpha_{hg}\right)$$

1D Simplification Results

$$T_{hw} = \frac{\left(1 + \frac{t}{\lambda} \alpha_c\right) T_{hg} + \frac{\alpha_c}{\alpha_{hg}} T_c}{\frac{\alpha_c}{\alpha_{hg}} + \frac{t}{\lambda} \alpha_c} \approx \frac{\left(1 + \frac{t}{\lambda} \alpha_c\right) T_{hg} + \frac{\alpha_c}{\alpha_{hg}} T_c}{\frac{\alpha_c}{\alpha_{hg}}} = \left(\frac{\alpha_{hg}}{\alpha_c} + \frac{t}{\lambda} \alpha_{hg}\right) T_{hg} + T_c$$

- Lowest possible **coolant temperature**.
- Low heat transfer coefficient at the hot side compared to the coolant heat transfer coefficient and the wall thermal impedance.
- Rule of thumb: $\alpha_c / \alpha_{hg} > 4$

1D Simplification Results

- Design conflict: High pressures are desired to maximize vehicle performance

But, with higher combustion chamber pressure:

- α_{hg} grows (Re grows due to higher density $\alpha \sim Re^{0.8} \sim \rho^{0.8} \sim p^{0.8}$)
- α_c grows similarly
- t/λ does not change

→ Higher wall temperature

$$T_{hw} \approx \left(\frac{\alpha_{hg}}{\alpha_c} + \frac{t}{\lambda} \alpha_{hg} \right) T_{hg} + T_c$$

Slightly sensitive to pressure (depends on cycle)

Very sensitive to pressure

- Highly non-linear phenomena can take place specially within the cooling channels where the fluid may transition from supercritical to transcritical state depending on the operating pressure.



Design

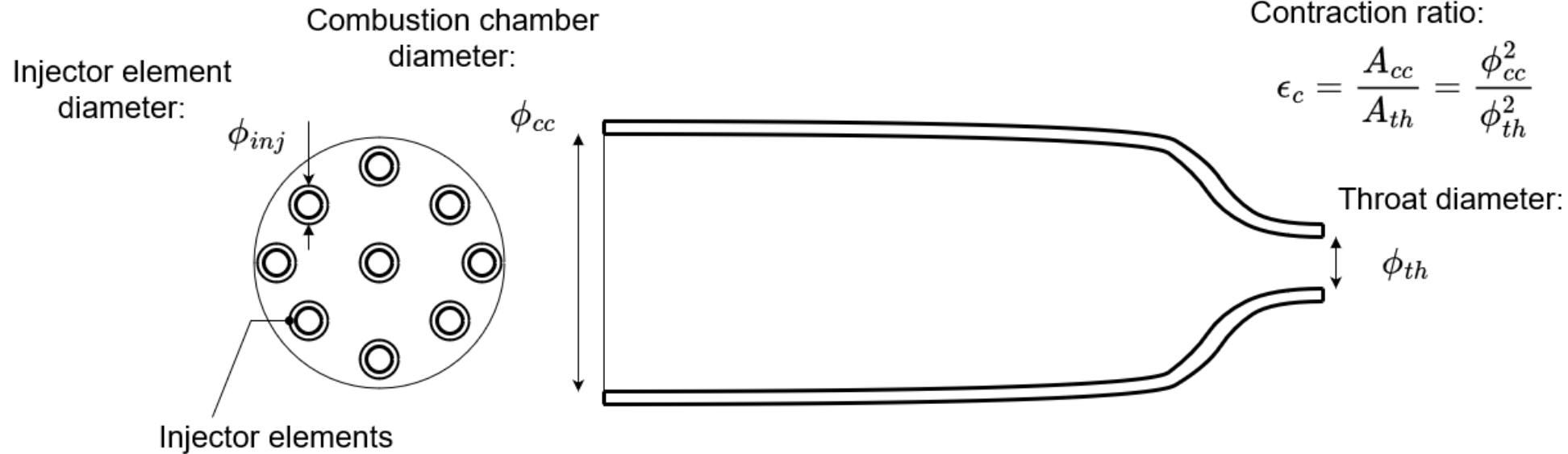
Assumptions

- The design of a rocket engine is a very dynamic process. There must be a continuous communication and interaction between all the systems, and multiple iterations are required. For example, improvements in the injection system can reduce the combustion chamber size and the required thrust.
- For simplicity, it will be assumed that the following parameters are inputs that we cannot alter:

- **Propellant combination and O/F**
- **Power cycle and injection pressure**
- **Required thrust**

In reality, these parameters can be modified during the combustion chamber development, but these effects will be neglected here.

Throat diameter

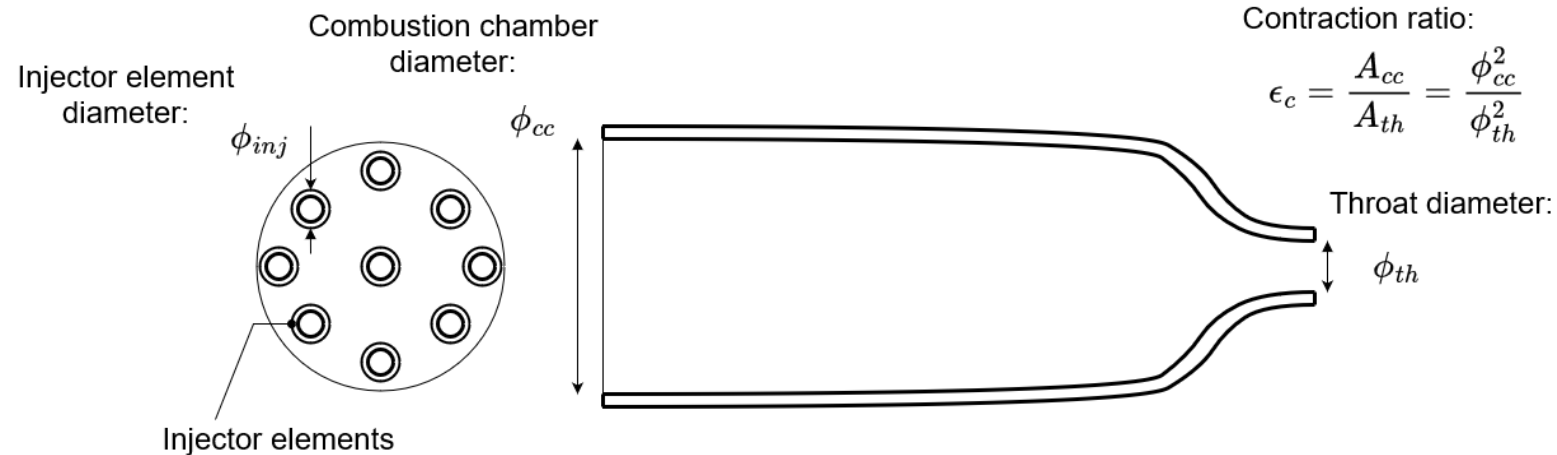


The throat diameter is given by the propellant combination, pressure and thrust.

It can hardly be modified.

$$c^* = \frac{p_c}{\dot{m}} A_{th} \rightarrow \phi_{th} = \sqrt{\frac{4 F}{\pi p_c C_F}}$$

Combustion chamber diameter



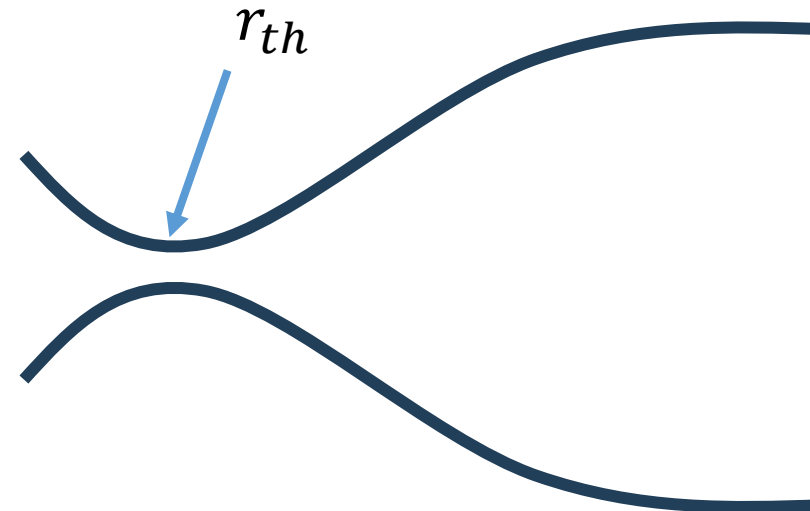
The contraction ratio ϵ_{cc} is chosen as small as possible to minimize the structural factor. However, excessively small values have the following disadvantages:

- With ϵ_{cc} too low the Mach number at the combustion chamber becomes close to unity and Pressure drop can become excessive.
- Lower residence time that can threaten η_{c^*}

In practice $\epsilon_{cc} \in [1.5, 6]$

Transition

- The convergent part of the nozzle It has a very small impact on the combustion performance. A smooth and simple geometry is commonly chosen to save manufacturing costs.
- The curvature at the throat can have a slight impact for the cooling power since it can generate secondary vortexes. However, this effect is very reduced (+10% additional cooling power)

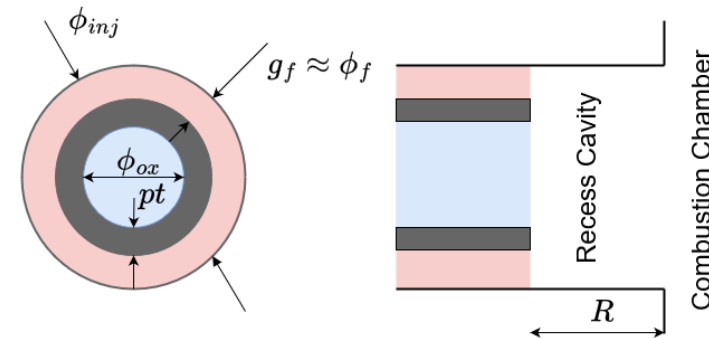


Injector geometry

- The main limiting factor are the manufacturing tolerances, with the current state of the art of technology the minimal realizable dimensions are in the order of 0.5 mm.
- The smaller, the holes the smaller the unmixedness scale and the lower the required residence time and L_{CC} .

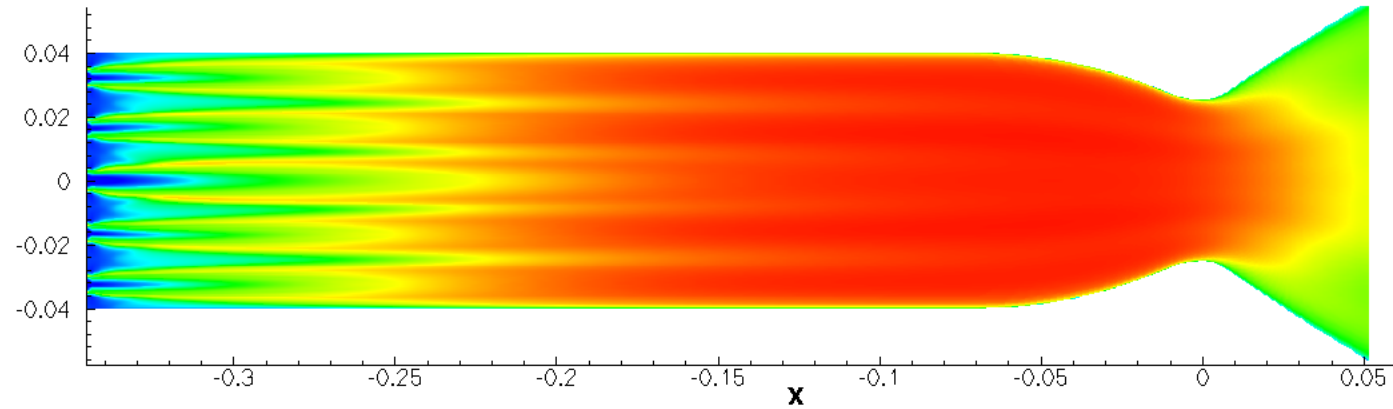
Decreasing the injector diameter increases the number of elements, which incorporates some disadvantages:

- Higher manufacturing costs.
- Higher inspection cost.
- Decreased structural robustness of the injection faceplate.

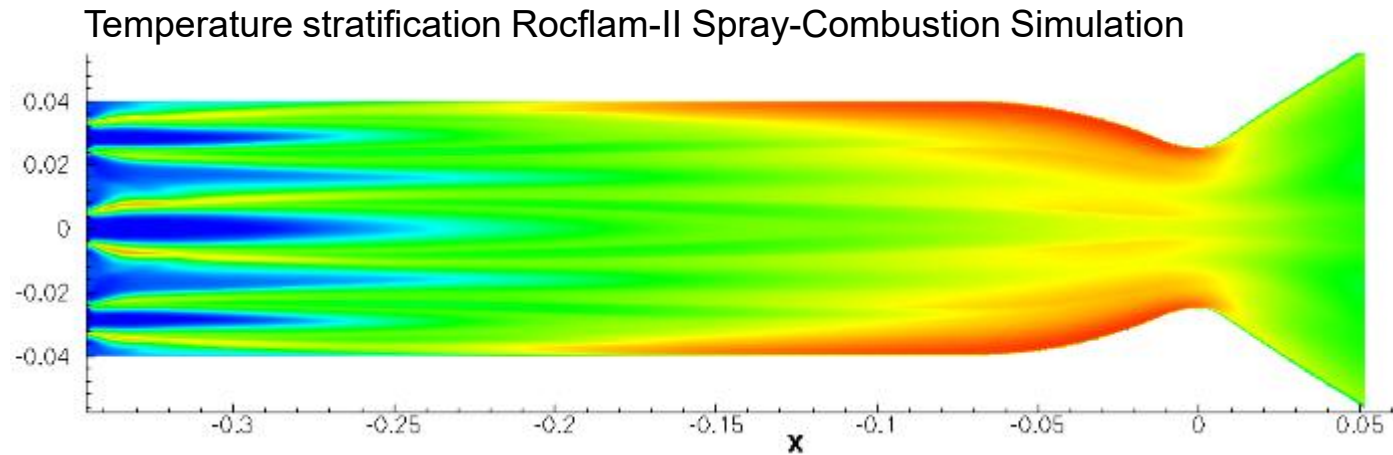


Injector geometry

- Shorter required L_{CC}
- Higher I_{sp} or lower σ
- Higher manufacturing cost.
- Higher inspection cost.
- More frail faceplate.



- Longer required L_{CC}
- Lower I_{sp} or higher σ
- Lower manufacturing cost.
- Lower inspection cost.
- More robust faceplate.



Injector geometry

Sufficient atomization and mixing of propellants is a key requirement for any injection system

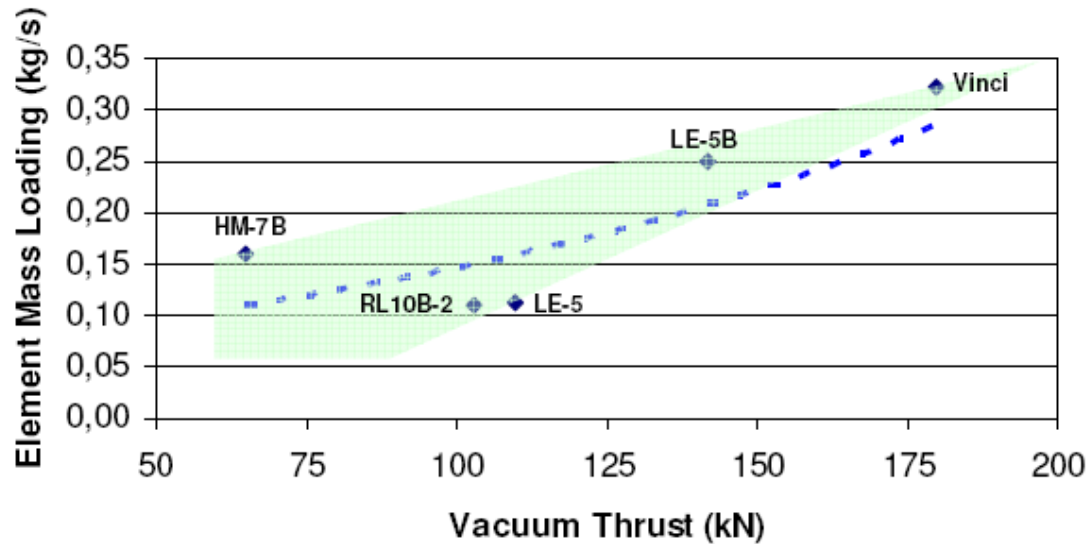
- Very efficient atomization through high initial shear forces provides for early mixing and combustion and yields high heat loads levels early on into combustion but complicates flame holding and stability
- Low initial shear rates yield poor atomization but generates favorable flame attachment and holding conditions, wall heat loads but bears the risk on lower combustion performance



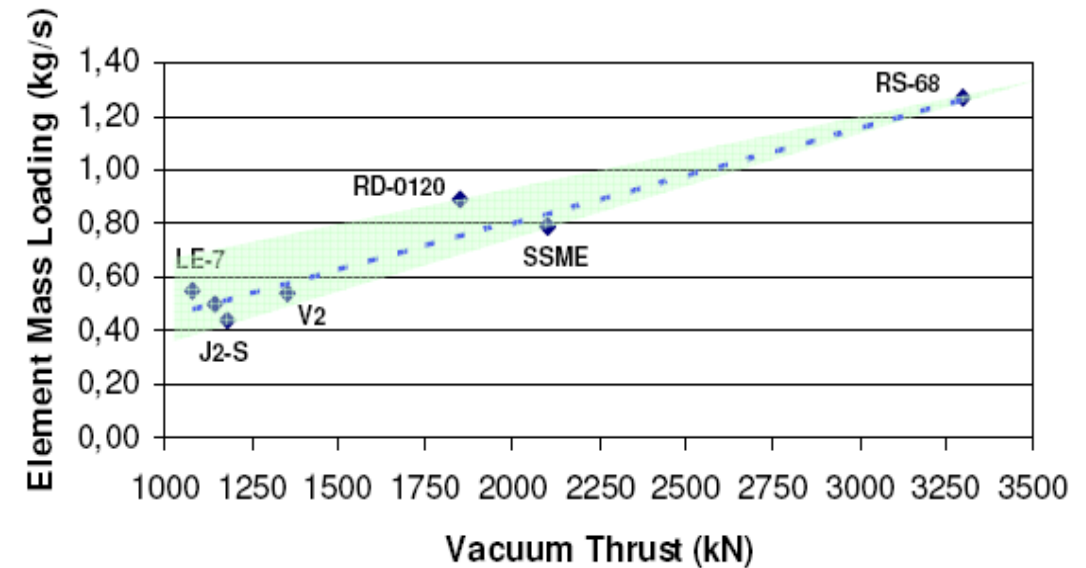
Injector design is always a compromise

Injector geometry

LOX/H₂ Upper Stage Engines



LOX/H₂ Booster and Main Stage Engines



- With growing thrust, performance is usually sacrificed for manufacturing costs and structural integrity of the injector faceplate.

Injector geometry: Pressure effects

There are three processes influencing the pressure evolution through the combustion chamber:

- **Friction losses (Usually negligible)**
- **Pressure rise due to cross-sectional area increase**

The increase of area from the injector manifold to the combustion chamber reduces the flow velocity. The kinetic energy is converted into thermal energy. If the propellants are compressible this, pressure and density rise accordingly. This effect can be relevant for gaseous propellants with a near ideal gas behavior.

- **Combustion pressure drop**

The thermal expansion due to the combustion process accelerates the flow, producing a pressure drop given by the Rayleigh line formula:

$$\frac{p_1}{p_0} = 1 - \gamma Ma_0^2 \left(\frac{u_1}{u_0} - 1 \right) \approx 1 - \gamma Ma_0^2 \left(\frac{T_P}{T_R} - 1 \right)$$

Whether the pressure drop/rise is beneficial or not highly depends on the situation. Generally, A 10-20 % pressure drop is desired to dampen any combustion instabilities. However, greater pressure losses can substantially downgrade the system performance due to the thrust reduction.

Combustion chamber length

The characteristic length L^* is used to compare systems with different thrust:

$$L^* = \frac{V_{cc}}{A_{th}} = L_{cc} \varepsilon_c$$

$$L^* = \Delta t_c \sqrt{\gamma} \left(\frac{2}{\gamma + 1} \right)^{\frac{\gamma+1}{2(\gamma-1)}} \sqrt{\frac{RT_c}{M}}$$

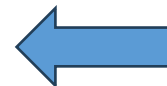
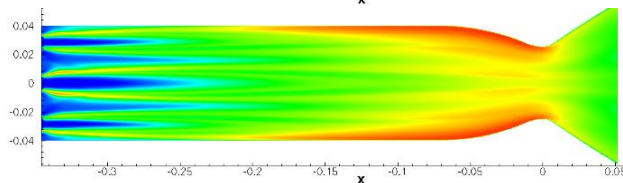
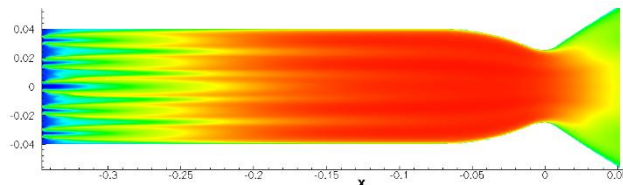
- necessary L^* (or. Δt_c) depends on
 - propellant combination
 - injection system
 - propellant temperatures
- large L^* results in
 - higher volume and weight
 - increased surface (cooling)
 - higher friction losses

Combustion chamber length

Estimated needed L^* depending on propellant combination.

Propellant combination	L^* [m]
LOX/GH ₂	0,6 – 0,7
LOX/LH ₂	0,7 – 1,0
LOX/Kerosene	1,0 – 1,3
NTO/N ₂ H ₄	0,8 – 1,0
NTO/UDMH	1,2
NTO/Aerozine	0,9

- These are rough estimates, and they can significantly vary depending on the actual conditions.
- In reality, what is roughly constant is the ratio L^*/ϕ_{inj} , hence the reference needed L^* is proportional to the injection length scales $L^* \sim \phi_{inj}$.
- Since the minimum manufacturable ϕ_{inj} is a constant everywhere, it follows that the reference L^* is constant as well.
- Multiple factors can impact the required L^* .



Same fuel but different needed L^*

Combustion chamber length

- **Injector diameter ϕ_{inj}**

If the injector diameter is reduced too much combustion instabilities can appear since the relative tolerances are worsened. In addition, the turbulent timescales can become smaller, leading to sporadic extinctions or lifted flames

- **Velocity ratio VR and momentum flux ratio J**

Velocity shears produce turbulence improving mixing. However, excessive velocity ratios can originate combustion instabilities.

- **Recess length R**

Recess improves mixing and enhances the stability at the flame anchoring point. Rule of thumb: For low recess ($R < 2\phi_{inj}$) the characteristic length can be reduced $\Delta L^* \approx aR$ with $a \in [3,10]$.

- **Oxidizer to fuel ratio O/F**

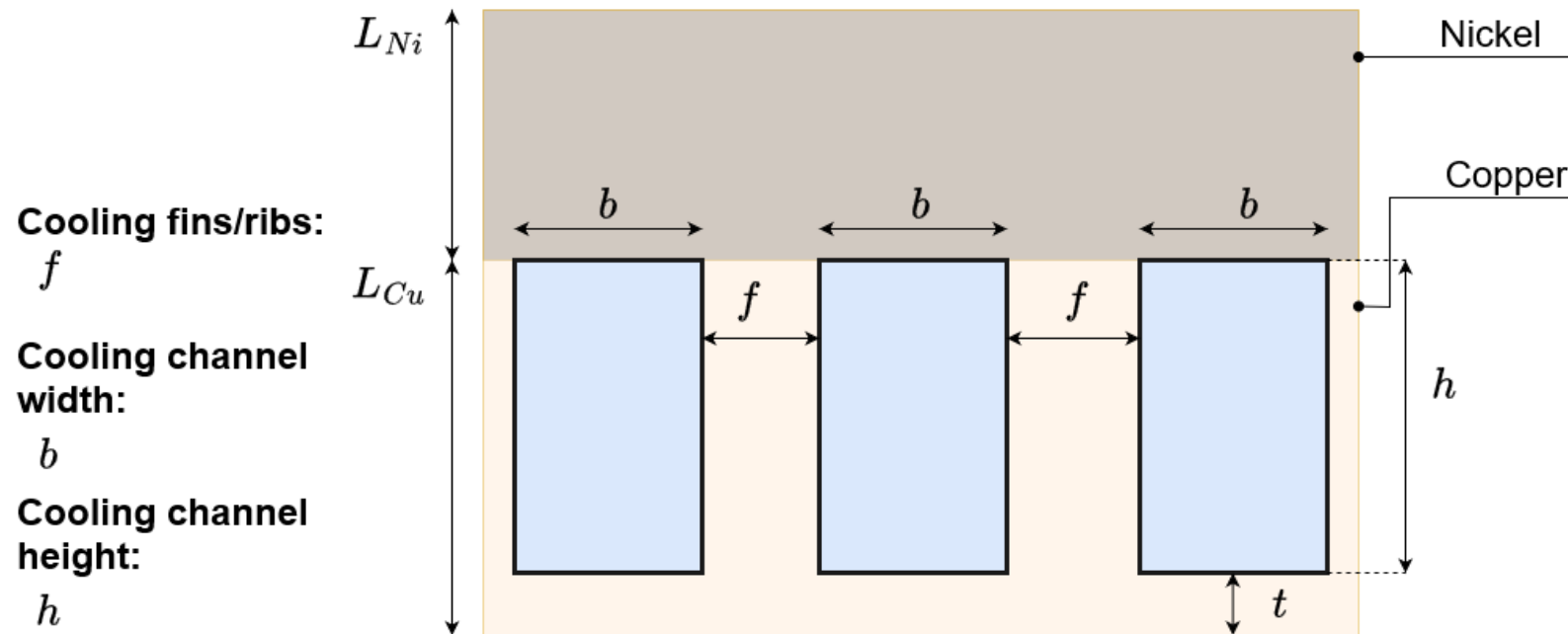
The closer the mixture is to stoichiometric the more length required, since the reactants in excess require no mixing.

- **Pressure and power cycle.**

Pressure speeds up chemical reactions. This effect is only relevant if chemistry is the limiting factor like with hydrazide or at low combustion chamber pressures $p_c < 10 \text{ bar}$

Cooling channels

- The cooling channel thickness t is manufactured as small as possible to minimize thermal impedance t/λ .
- With today's technology $t_{min} \in [0.7 \text{ mm } 1.2 \text{ mm}]$.



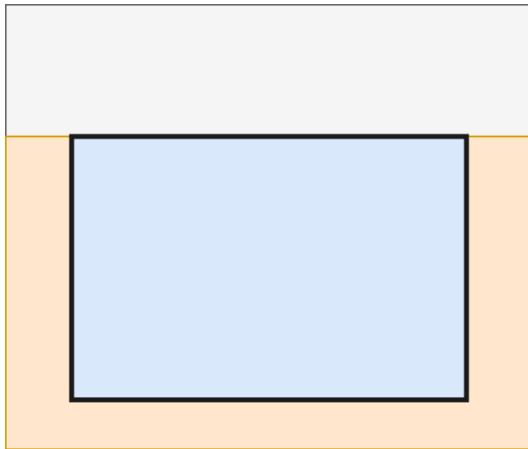
Cooling channels

- The cooling channels geometry are essentially a tradeoff between pressure drop and cooling power.
- Here we study rectangular geometries for simplicity but oval and circular have also been attempted although they are more expensive.

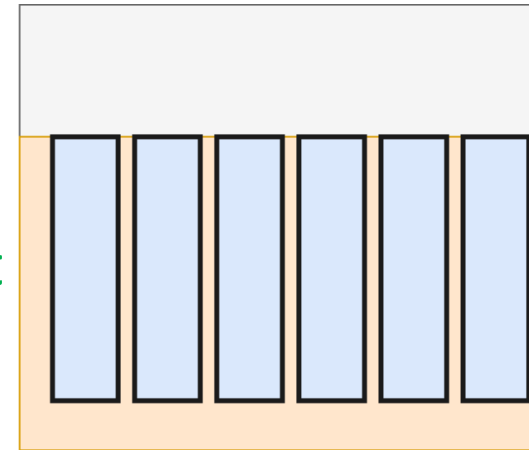
At Identical \dot{m} :

$$\Delta p \sim \frac{1}{\phi_H}$$

$$\alpha \sim \frac{Re^{0.8}}{\phi_H}$$



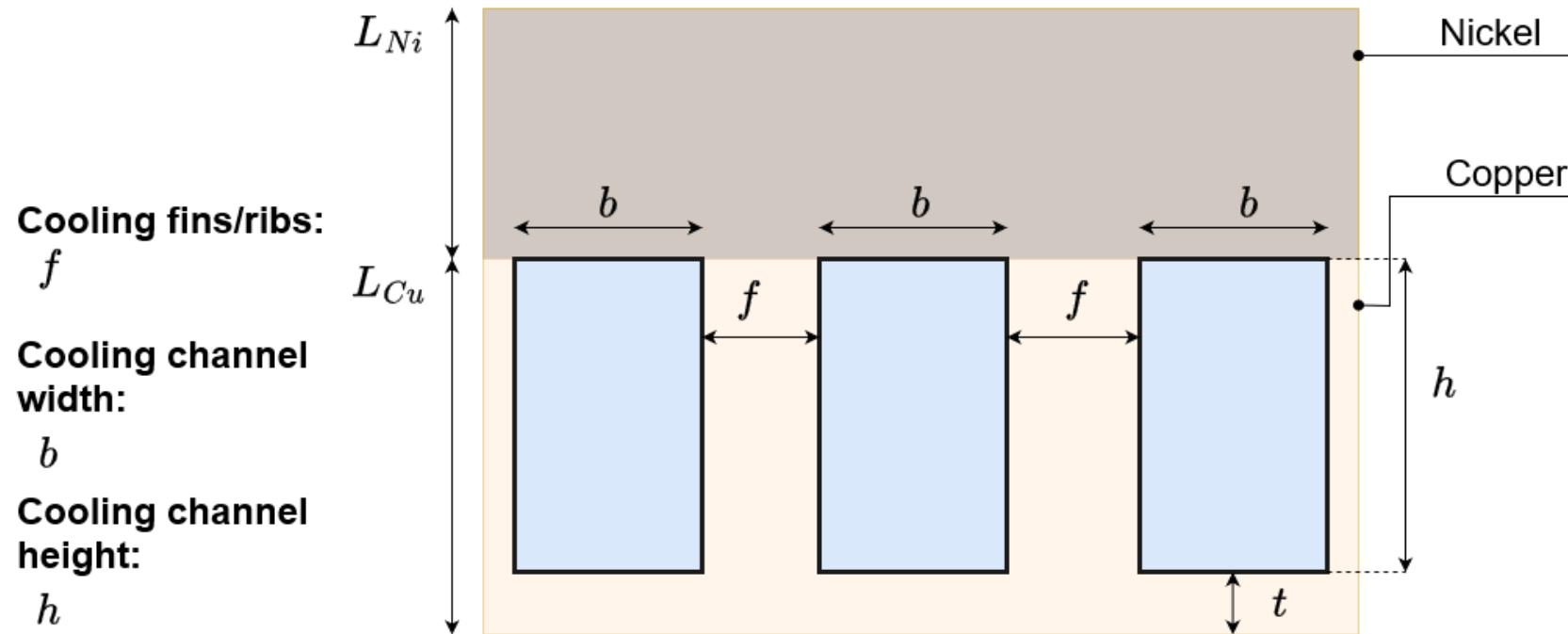
Higher Re and Nu
 Lower pressure losses
 Lower manufacturing cost
 Lower contact length
 Lower α



Lower Re and Nu
 Higher pressure losses
 Higher manufacturing cost
 Larger contact length
 Slightly higher α
 Significantly higher cooling capacity.

Cooling channels

- Nickel length it is chosen by manufacturing constrains and to ensure structural integrity. The determination of the optimal L_{Ni} is out of the scope of this lecture.



What you should not forget

- Geometrical parameters of typical combustion chamber and injector geometries.
- Injector typologies with their advantages and disadvantages.
- Regenerative cooling and heat transfer basic principles.
- Factors influencing the operating life of a combustion chamber.
- Drivers for the combustion chamber geometry. Sensitivity of performance, cost and weight to injector configuration.